Molecular Pharmacology Fast Forward. Published on July 21, 2009 as doi: 10.1124/mol.109.056838
This article has not been copyedited and formatted. The final version may differ from this version.

MOL # 56838

Inhibition of human two-pore domain K^+ channel TREK1 by local anesthetic lidocaine: negative cooperativity and half-of-the-sites saturation kinetics.

Tapan K. Nayak, Harinath S., Nama S., Somasundaram K., Sikdar S.K.§

[TKN, HS, SK]Molecular Biophysics Unit, [NS, KS]Microbiology and Cell Biology, Indian Inst. of Science, Bangalore-560012

Molecular Pharmacology Fast Forward. Published on July 21, 2009 as DOI: 10.1124/mol.109.056838
This article has not been copyedited and formatted. The final version may differ from this version.

Running title page

a) Running title: Negative cooperativity in lidocaine inhibition of hTREK1

b) Corresponding author§

Sujit K Sikdar,

Molecular Biophysics Unit,

Indian Inst. of Science,

Tel: 91-80-2293 3220

Fax: 91-80-2360 0535

E-mail: sks@mbu.iisc.ernet.in

c) Number of text pages: 49

Number of tables: 0

Number of figures: 11

Number of references: 41

Number of words:

Abstract: 231

Introduction: 747

Discussion: 1450

d) Non-standard abbreviations:

CTD: Carboxyl terminal domain

NTD: Amino terminal domain

pdf: Probability density function

Molecular Pharmacology Fast Forward. Published on July 21, 2009 as DOI: 10.1124/mol.109.056838
This article has not been copyedited and formatted. The final version may differ from this version.

Abstract

TWIK-related K^+ channel TREK1, a background leak K^+ channel has been strongly implicated as the target of several general and local anesthetics. Here, using the whole-cell and single-channel patch-clamp technique, we investigated the effect of lidocaine, a local anesthetic on the human TREK1 (hTREK1) channel heterologously expressed in HEK 293 cells by an adenoviral mediated expression system. Lidocaine, at clinical concentrations, produced reversible, concentration-dependent inhibition of hTREK1 current with IC_{50} of 180 μM by reducing the single-channel open probability and stabilizing the close state. We have identified a strategically placed unique aromatic couplet (Tyr352 and Phe355) in the vicinity of the PKA phosphorylation site, Ser348 in the C-terminal domain (CTD) of hTREK1 which is critical for the action of lidocaine. Further, the phosphorylation state of Ser348 was found to have a regulatory role in lidocaine mediated inhibition of hTREK1. Interestingly, we observed strong inter-subunit negative cooperativity (Hill coefficient 0.49) and half-of-the-sites saturation binding stoichiometry (half reaction order) for the binding of lidocaine to hTREK1. Studies with the heterodimer of wt-hTREK1 and Δ119 C-terminal deletion mutant ($hTREK1_{wt}$-Δ119) revealed that single CTD of hTREK1 was capable of mediating partial inhibition by lidocaine, but complete inhibition necessitates the cooperative interaction between both the CTDs upon binding of lidocaine. Based on our observations, we propose a model that explains the unique kinetics and provides a plausible paradigm for the inhibitory action of lidocaine on hTREK1.

Molecular Pharmacology Fast Forward. Published on July 21, 2009 as DOI: 10.1124/mol.109.056838
This article has not been copyedited and formatted. The final version may differ from this version.

Introduction

The molecular mechanism of local anesthetic action on voltage-gated sodium (Na^+) channels and the resulting blockade of action potential propagation are well documented (Ragsdale et al., 1994). Besides the voltage-gated Na^+ channels, other ion channels and receptors have been implicated in the action of local anesthetics (Cuveas and Adams, 1994; Nishizawa et al., 2002). Increasing evidences suggest that local anesthetics potently block potassium current (Carmeliet et al., 1986) which potentiates local anesthetic-induced inhibition of action potential firing (Drachman and Strichartz, 1991). In heterologous and native preparations, several voltage-gated potassium channels, including $hK_v1.5$, $K_v2.1$, K_vLQT, and G protein-coupled inward rectifying K^+ channels have been identified as targets of local anesthetics (Gonzalez et al., 2001; Kindler et al., 2003; Zhou et al., 2001). Modulation of K^+ channel function, by local anesthetics may influence the transmission of sensory impulses by altering the resting membrane potential, repolarization after an action potential, and firing frequency of a neuron (Komai and McDowell, 2001). These studies indicate that the effects of local anesthetics in neural tissue may extend beyond the known direct actions on voltage-gated sodium channels (Kindler and Yost, 2005).

Recently, a new super family of K^+ channels, the tandem pore domain K^+ channels (K_{2P} channels) has been cloned and characterized (Honore, 2007). It was found to contribute to background or leak K^+ conductances involved in maintaining the resting membrane potential and firing pattern of excitable cells (Lesage et al., 1996). These channels are modulated by a wide array of cellular lipids and pharmacological agents, including polyunsaturated fatty acids, second messengers, and general anesthetics (Honore, 2007). Most of the members of this family are expressed widely in the central and peripheral nervous system. Local anesthetics have been identified as potent inhibitors of the K_{2P} channels causing membrane depolarization, which in

Molecular Pharmacology Fast Forward. Published on July 21, 2009 as DOI: 10.1124/mol.109.056838
This article has not been copyedited and formatted. The final version may differ from this version.

turn promotes switching of voltage-gated Na^+ channels to open and inactivation states, thereby increasing their affinity for local anesthetics. Moreover, increases in neuronal excitability due to inhibition of K_{2P} channels may contribute to the cardiotoxic and excitotoxic side effects of local anesthetics (Kindler et al., 2003). Bupivacaine, one of the most potent and toxic local anesthetics clinically used, inhibits the K_{2P} channels, TASK1 and TREK1 at clinically relevant concentrations achieved by intravascular injection (~20 μM) (Punke et al., 2003; Kindler and Yost, 2005). Lidocaine, an amide local anesthetic was found to inhibit K_{2P} channel TASK2 at clinical doses (Kindler et al., 2003). However, the effect of lidocaine on human TREK1, the most thoroughly studied K_{2P} channel, has not been investigated.

Lidocaine, traditionally used as a local anesthetic and an anti-arrhythmic drug, also exerts several unwarranted effects such as neurotoxicity, bronchial hyper-responsiveness, ototoxicity (ringing paresthesia), and convulsions at higher concentration in various clinical settings (Benkwitz et al., 2003). On the other hand, CNS excitation, leading to seizures, has been partly attributed to local anesthetic action on K_{2P} channels, especially TREK1 (Kindler and Yost, 2005). Lidocaine has also been known to have inhibitory effects on neurophysiologic responses evoked by Aδ and C fibers in the dorsal root ganglion (Ness, 2000). Human tissue distribution assays indicate a prominent expression of TREK1 in dorsal root ganglia and the spinal cord. Furthermore, TREK1 has also been strongly implicated in pain perception and can be activated by nociceptive stimuli, including pressure and heat (Honore, 2007). Above evidences suggest a possible interaction of lidocaine with the TREK1 channel, which might explain its clinical actions.

In the present work, we investigated the effect of lidocaine on human TREK1 channels. In heterologous expression system, at whole-cell as well as single-channel level, lidocaine produced

Molecular Pharmacology Fast Forward. Published on July 21, 2009 as DOI: 10.1124/mol.109.056838
This article has not been copyedited and formatted. The final version may differ from this version.

rapid and reversible inhibition of hTREK1. Experiments with the deletion mutants revealed the importance of the distal 89 residues of the C-terminal domain (CTD) of hTREK1 in mediating the effect of lidocaine. Furthermore, from site-directed mutagenesis studies, we identified a sub-domain in the CTD comprising an aromatic couplet, Tyr352 and Phe355, adjacent to the PKA phosphorylation site Ser348, which was critical for the inhibitory action of lidocaine. Interestingly, we also observed strong negative cooperativity and half-of-the-sites saturation kinetics for the interaction of lidocaine with the channel. Kinetic analysis of the heterodimer of wild-type hTREK1 and CTD deletion mutant provided insight into the unique kinetic mechanism of lidocaine binding to hTREK1.

In conclusion, our results suggest that lidocaine, at clinical concentrations, potently inhibits the hTREK1 channel by binding to a putative lidocaine binding site in the CTD of hTREK1. Further, binding of lidocaine to the CTD of the two monomers of hTREK1 induces an inter-subunit negative cooperativity at single-channel level.

Molecular Pharmacology Fast Forward. Published on July 21, 2009 as DOI: 10.1124/mol.109.056838
This article has not been copyedited and formatted. The final version may differ from this version.

Materials and Methods

Cell culture and molecular biology reagents

HEK 293 (human embryonic kidney) cells were maintained in DMEM F12-HAM, supplemented with 10 % fetal bovine serum (v/v), 1 % antibiotic-antimycotic (Sigma) and Gentamicin (50 μg/ml) (Sigma) in a humidified incubator with 5 % CO_2. cDNA encoding the human TREK1 (hTREK1) channel (Gen Bank accession no: AF004711) cloned in the mammalian expression vector pRAT (kindly donated by Prof. Steve A.N. Goldstein, Yale University medical school) was utilized for the construction of recombinant hTREK1 adenovirus. The AdEasy1 adenoviral vector system including the pAdTrack-CMV (shuttle vector), pAdEasy-1 and the electro-competent cells of BJ5183 strain of *E.coli* was a generous gift from Prof. Bert Vogelstein (John Hopkins Oncology Centre). The C-terminal deletion mutants of hTREK1 (Δ89 and Δ119 hTREK1) were constructed by PCR mutagenesis as described previously (Harinath and Sikdar, 2004) and the S348A mutant of hTREK1 was a generous gift from Prof. Steve A.N. Goldstein, Yale University medical school. The other site-directed mutagenesis such as the S348D, S366A and Y352A/F355A were performed with a QuikChange™ kit (Stratagene) and mutations were verified by DNA sequencing which are illustrated in Fig. S4. The primers for the PCR mutagenesis are listed in the supplementary text. For electrical recordings from the mutants (deletion as well as substitution), the HEK 293 cells were transiently transfected with the mutant hTREK1 cDNA using the calcium phosphate method. Briefly, the complex of calcium and DNA (0.5 μg cDNA of the mutant hTREK1 along with 0.33 μg of EGFP) was added to HEK 293 cells cultured in 35 mm dishes. After 4 hrs of incubation, the cells were replenished with fresh medium following a brief osmotic shock using 10 % glycerol in PBS. The cells were used for

Molecular Pharmacology Fast Forward. Published on July 21, 2009 as DOI: 10.1124/mol.109.056838
This article has not been copyedited and formatted. The final version may differ from this version.

electrophysiological experiments after 24-30 hrs of transfection. Transfected cells were identified by the green fluorescence from cells expressing EGFP in a standard fluorescence microscope. For the study of the heterodimer, wt-hTREK1 and Δ119 mutant cDNA were cotransfected in HEK 293 cells in equimolar ratio by the calcium phosphate method (Czirjak and Enyedi, 2002).

Construction of recombinant hTREK1 adenovirus and gene transfer

We employed the efficient homologous recombination machinery of *E.coli* using the AdEasy-1 system for the construction of adenovirus as described earlier (He et al., 1998). Briefly, the *SalI/XbaI* restriction fragment from the pRAT-hTREK1 was cloned into the shuttle vector pAdTrack-CMV at the corresponding sites. The resultant plasmid (pAdTrack-hTREK1) was linearized with *PmeI* and co-transformed with the adenoviral backbone vector pAdEasy-1 into the BJ5183 cells by electroporation. Homologous recombinants containing the hTREK1 cDNA were detected by restriction digestion and agarose gel electrophoresis. Recombinant hTREK1 adenovirus (pAd-hTREK1) was then transformed into *E.coli* DH10B cells for large-scale amplification. The *PacI*-digested pAd-hTREK1 was transfected into HEK 293 cells by classical calcium phosphate method and the hTREK1 adenovirus was expanded, purified and titered as described earlier (He et al., 1998). The recombinant adenovirus encoding green fluorescent protein (Ad-GFP) was used as control. The efficiency of packaging and amplification of adenovirus could be determined by GFP expression.

For adenoviral infection, subconfluent (80-90 % confluency) HEK 293 cells were incubated with Ad-hTREK1 or Ad-GFP at a multiplicity of infection (MOI) of 15-20 at 37 ^{0}C in normal growth medium. After 2 hrs of incubation, the infection medium was replaced with fresh medium and the cells were further incubated for 20-30 hrs. Subsequently, the infected cells were utilized for

Molecular Pharmacology Fast Forward. Published on July 21, 2009 as DOI: 10.1124/mol.109.056838
This article has not been copyedited and formatted. The final version may differ from this version.

quantitative real time PCR or regular electrophysiological experiments. Most of the electrophysiology experiments were carried out in HEK 293 cells infected with Ad-hTREK1 unless otherwise mentioned.

RT PCR and quantitative real time PCR

Total cell RNA was prepared from the infected HEK 293 cells using the TRIzol reagent (Aldrich). First strand cDNA was synthesized using the ProtoScript cDNA synthesis kit (NEB) employing the MuLV reverse transcriptase and random primers. The reverse transcription product was amplified with hTREK1 specific primers (forward: 5'-GCTGTCCTGAG CGGATCCGGAGATTGGCTCCG-3', reverse: 5'-GGTTTAGTGGTAGTCGACTTATTAATT TGATGTTCTCAATCAC-3'; Sigma) and specific primers for the human GAPDH (Glyceraldehyde 3-phosphate dehydrogenase), which served as the positive control.

Quantitative real-time PCR was performed using SYBR Green chemistry in 96-well optical plates on an ABI prism 5700 sequence detector (Applied Biosystems, Foster City, CA). The standard curves were generated by the regression analysis of the mean values of three multiplex PCRs for the $\log_{10}$ diluted cDNA. Real time PCR was run for hTREK1 and human β-actin using cDNA corresponding to 200 ng total cell RNA and gene-specific primers (specified above) using the DyNamo master mix (NEB) as per the manufacturer's instructions. Before quantification of real time data, the specificity of the amplified product was examined by agarose gel electrophoresis and by dissociation curve analysis. For comparison of gene expression levels, all quantification were normalized to endogenous β-actin levels to account for variability in the initial concentration and quality of total RNA in the conversion efficiency of the reverse

transcriptase reaction. The standard-curve method was used for quantification and normalization of cDNA amplification.

Electrophysiology, anesthetic application and data analysis

Electrophysiological recording was performed using an EPC8 patch-clamp amplifier (*HEKA Elektronik, Germany*). Whole-cell current and membrane potential were measured with the voltage-clamp and current-clamp methods, respectively, of the patch-clamp technique. Borosilicate micropipettes of 2-5 MΩ resistance were used for whole-cell recordings. Single-channel current recordings were acquired in the excised inside-out configuration of patch-clamp using fire polished micropipettes of 5-10 MΩ resistance, whose tips were coated with *Sylgard (General Electric)* to reduce capacitive noise (Hamill et al., 1981). The recordings were filtered at 3 KHz using a 7-pole Bessel filter (~3 dB), digitized using an LIH 1600 A/D converter interface *(HEKA Electronik, Germany)* at a sampling rate of 20 kHz and analyzed offline by the Pulse *(HEKA Electronik, Germany)* and TAC software (*Bruxton Corp, Seattle, Washington*). In experiments using the excised patches, pipette and bath solutions contained: (mM) 155 KCl, 5 EGTA, 3 $MgCl_2$, 10 HEPES (pH adjusted to 7.4 with KOH). In whole-cell recordings, bath solution contained: (mM) 145 NaCl, 2.5 KCl, 3 $MgCl_2$, 1 $CaCl_2$, and 10 HEPES (pH 7.4; adjusted with NaOH), whereas the pipette was filled with the intracellular solution containing (mM) 150 KCl, 3 $MgCl_2$, 5 EGTA, and 10 HEPES (pH 7.4; adjusted with KOH). All recordings were done at room temperature and by holding the cell at -80 mV.

Whole-cell hTREK1 current was elicited by either a voltage ramp (300 ms) or incrementing voltage steps (50 ms) from -100 to 60 mV (inter-pulse interval of 5 s) unless specified. The time-dependent component was obtained from the activation time course of the whole-cell current by

Molecular Pharmacology Fast Forward. Published on July 21, 2009 as DOI: 10.1124/mol.109.056838
This article has not been copyedited and formatted. The final version may differ from this version.

fitting it with a mono-exponential function of the form $y = y_0 + a\,[1-\exp(-x/\tau)]$. On the other hand, the inhibition time course was fitted with one or two decaying exponential functions of the form $y = y_0 + a*\exp(-x/\tau)$ to obtain the decay time constant for lidocaine mediated inhibition. Single-channel current recording was acquired in gap free mode from a holding pipette potential of 0 mV. Single-channel events were detected by setting a threshold at half the maximum open channel current amplitude of the major conductance state (Colquhoun and Sigworth, 1983). Single-channel current amplitude was determined by constructing amplitude histograms and fitting with Gaussian distributions. Unitary current amplitudes obtained at different membrane potentials were used to plot the current-voltage (I-V) relationship. hTREK1 channel activity in a patch was expressed quantitatively as the NP_o, i.e. the product of the number of channels *(N)* in a patch and the probability that the channel would be in the open state, P_o. The NP_o was calculated by the relative area under all points amplitude histogram and expressed as follows:

$$NPo = \sum_{i=1}^{N} i.\,A_i / \sum_{i=0}^{N} A_i \quad \text{...} \; (1)$$

where, *A* is the area under the Gaussian curve and *i* is the number of active channels in a given recording fragment. For the NP_o analysis, it was assumed that the channels in a patch are identical and independent. The relative change in NP_o was obtained by measuring the average NP_o from approximately 1-2 minute recordings. Dwell time distribution histograms were obtained by plotting the number of events against appropriately binned time interval. While constructing the dwell time histograms the missed events were appropriately taken into account (Colquhoun and Sigworth, 1983). A maximum likelihood method was used to fit the histograms with a sum of exponential probability density functions (pdfs) to yield the mean dwell times or the time constants ($\tau_{open,}$ τ_{close}) (Colquhoun and Sigworth, 1983).

Molecular Pharmacology Fast Forward. Published on July 21, 2009 as DOI: 10.1124/mol.109.056838
This article has not been copyedited and formatted. The final version may differ from this version.

Stock solutions of the local anesthetic, lidocaine (10 mM; Sigma), 2, 2, 2-trichloroethanol (TCE, 10 mM; Aldrich) and QX314 (10 mM) (lidocaine N-ethyl bromide; kindly provided by Dr. Rune Sandberg, Astra Pain Control, Sweden) were freshly prepared in the extracellular saline solution. The stock solutions of forskolin (Sigma, 10 mM), the protein kinase A (PKA) activator, and KT 5720 (Alomone labs, 5 mM), PKA inhibitor, were prepared in DMSO. Test solutions of the drugs were prepared by diluting the stock solution in the extracellular solution. The final concentration of DMSO was less than 0.1 % in the test solutions, which was found to have no effect on the channel. The anesthetic and the drug solutions were applied locally to the cells or very close to the patch by either pressure ejection (*Medical Systems Corp., NY*) or by a hydrostatic pressure driven fast perfusion device controlled by six channel valve controller (*VC-6; Warner Instruments Corp., CT*). During application of the anesthetic, the bath was continuously perfused with the extracellular solution. For dose response experiments, NP_o of hTREK1 channel was measured at -60 mV in the presence and absence of the drug over a period of 2 minutes. The percent change in the NP_o by a drug was quantified at various test concentrations according to the following equation,

$$\% \text{ change} = 100\,[(NP_{oDrug} - NP_{oControl})/NP_{oControl}] \quad (2)$$

where NP_{oDrug} and $NP_{oControl}$ were the measured NP_o after and before application of the drug respectively. Steady-state concentration response of hTREK1 was fitted to the Hill equation of the form $y = (ax^b)/(c^b + x^b)$; where y = hTREK1 response, x = drug concentration, a = maximal response, b = Hill coefficient, and c = half maximal inhibitory or activating concentration. Single-channel currents, in presence of the anesthetic, were recorded only in the steady state. All results have been presented as the mean ± standard error (SEM). Results were considered

Molecular Pharmacology Fast Forward. Published on July 21, 2009 as DOI: 10.1124/mol.109.056838
This article has not been copyedited and formatted. The final version may differ from this version.

significant when $p < 0.05$ in the Student's *t*-test or non-parametric test such as the Mann-Whitney test.

Molecular Pharmacology Fast Forward. Published on July 21, 2009 as DOI: 10.1124/mol.109.056838
This article has not been copyedited and formatted. The final version may differ from this version.

Results

Expression of hTREK1 in HEK 293 cells

HEK 293 cells infected with Ad-hTREK1 exhibited high level of hTREK1 mRNA expression, whereas the uninfected and control adenovirus (Ad-GFP) treated cells failed to induce the expression of hTREK1. Figure 1a and b show the SYBR Green real time PCR kinetic data traces of hTREK1 and the corresponding dissociation curves respectively. Melting temperature higher than 75^0C indicates no primer-dimer formation (Fig. 1b), whereas a single band of desired size in agarose gel electrophoresis (~0.4 kb) confirms the specificity of amplification of hTREK1 in the real-time PCR reaction (Fig. 1c). Fig. 1d illustrates the fold increase in the expression of hTREK1 in the Ad-hTREK1 infected cells. The expression of the hTREK1 mRNA was accompanied by enhanced whole-cell hTREK1 channel current which was assayed by patch-clamp experiments.

Lidocaine inhibits whole-cell hTREK1 current

hTREK1, when expressed in infected HEK 293 cells formed functional channels with kinetics similar to that described earlier (Harinath and sikdar, 2004). In physiological K^+ gradient an outwardly rectifying, non-inactivating, time-dependent current progressively developed upon depolarization, which was absent in uninfected cells and Ad-GFP infected cells (Fig. S1a and b). We evaluated the sensitivity of hTREK1 to varying concentrations of the local anesthetic, lidocaine (10 μM-5 mM). The reported plasma concentration of lidocaine is estimated between 20-30 μM when lidocaine is administered intravenously for arrhythmia or neuroprotection (Johnson et al., 2004) whereas local anesthetic induced seizure and cardiovascular collapse ensue when the plasma concentrations of lidocaine exceeds 50 μM (DeToledo, 2000). During spinal or

Molecular Pharmacology Fast Forward. Published on July 21, 2009 as DOI: 10.1124/mol.109.056838
This article has not been copyedited and formatted. The final version may differ from this version.

epidural anesthesia, lidocaine concentration in the CSF normally reaches as high as 10 mM for the first 15 minutes after injection (Johnson et al., 2004). Thus, the steady state concentration of lidocaine in the CNS and peripheral nervous system in various clinical conditions commensurate with the range we have used in the current study. In this physiological concentration range, lidocaine was found to inhibit the whole-cell hTREK1 current in a dose dependent manner. Fig. 2a illustrates hTREK1 current elicited by ramp changes in membrane potential (-100 to 100 mV) on application of increasing concentrations of lidocaine. The current inhibited by lidocaine reversed close to -90 mV (Fig. 2a), as predicted by the Nernst equation for a purely K^+ selective channel. On washing out, the inhibitory effect of the anesthetic could be reversed (Fig. 2b). The inhibition of hTREK1 current upon application of varying concentrations of lidocaine was described by the Hill equation (methods). The half-maximal inhibitory concentration (IC_{50}) and the Hill coefficient (α_H) were estimated to be 207 ± 31 μM and 0.49 ± 0.08 respectively (Fig. 2c). A Hill coefficient less than 1 indicates negative cooperativity in the interaction of lidocaine with the hTREK1 channel.

Inhibition of hTREK1 channel current was expected to result in membrane depolarization. Consistent with this, lidocaine caused an immediate and reversible depolarization of the membrane of cells expressing hTREK1 channels (Fig. 2d). At a concentration of 0.5 mM, lidocaine caused membrane depolarization by 14.7 ± 1.2 mV (n = 5). The hTREK1 current has two distinct components, (i) an instantaneous and (ii) a time and voltage-dependent component. The time-dependent component was quantified by fitting the activation time course with mono-exponential function (methods; Fig. 2e). Lidocaine, at all test concentrations, caused significant inhibition ($p < 0.01$, n = 7, Mann-Whitney test) of both the time-dependent and non-time-dependent components of hTREK1 current (77.8 ± 7.3 % and 57.6 ± 11.4 % respectively in

Molecular Pharmacology Fast Forward. Published on July 21, 2009 as DOI: 10.1124/mol.109.056838
This article has not been copyedited and formatted. The final version may differ from this version.

presence of 1 mM lidocaine, n = 7; Fig. 2f) compared to the control (0 mM lidocaine). Voltage dependence of inhibition was analyzed by quantifying the reduction in whole-cell current amplitude at three different membrane potentials: -40, 0 and 40 mV at a concentration of 0.1 mM lidocaine (Fig. 2g). Inhibition of hTREK1 channels was, however, voltage-independent (43.7 ± 3.6 % , 40.7 ± 1.5 %, and 40.5 ± 1.3 % at -40 mV, 0 mV and 40 mV respectively; n = 4, $p > 0.05$; Mann-Whitney test; Fig. 2g).

Inhibition of single hTREK1 channel by lidocaine

The inhibitory effect of lidocaine was observed in excised inside-out patches containing single hTREK1 channels. Fig. 3a (i) shows the representative single hTREK1 channel current traces evoked at different membrane potentials in symmetrical K^+ gradient in presence of 3 mM Mg^{2+} in the bath. The single-channel current reversed at 0 mV and exhibited mild outward rectification (Fig. 3a, b), which are characteristic of the hTREK1 channel. The single-channel I-V relationships of hTREK1 in physiological and symmetrical gradients of K^+ were plotted by measuring the unitary current amplitudes at varying membrane potentials (Fig. 3c), which show the shift in reversal potential of hTREK1 from ~-84 mV to 0 mV upon changing the external K^+ concentration from 2.5 to 150 mM. Above observation confirms the K^+ selectivity of the hTREK1 channel isoform we used for our experiments. The slope conductance measured from the linear part of single channel I-V relation was found to be 95.7 ± 9.4 pS (n = 7), which is in agreement with earlier observations (Bockenhauer et al., 2001; Honore, 2007). Recently, it was reported that alternative translation initiation leading to generation of splice variants with shorter N-terminal domains result in channels with variable conductance and increased permeability to Na^+ (Thomas et al., 2008; Simkin et al., 2008). However, in our hands, all the hTREK-1 channel

Molecular Pharmacology Fast Forward. Published on July 21, 2009 as DOI: 10.1124/mol.109.056838
This article has not been copyedited and formatted. The final version may differ from this version.

activities observed were K^+ selective and had similar single-channel conductance as mentioned above (Fig. 3c)**.** Thus, the experimental results presented here on the effects of lidocaine on hTREK-1 are most likely on the single isoform of hTREK-1 channels with an intact N-terminal domain (NTD)**.** Human TREK1 is a known mechano-sensitive channel. On application of negative pressure in excised patches, the open probability of single hTREK1 channels increased significantly (Fig. 3d). This was used as a positive test to identify the hTREK1 channels in excised patches.

Fig. 4a illustrates the single hTREK1 channel activity elicited at –60 mV in control, in presence of lidocaine and after wash-out. It shows that lidocaine reversibly and in a concentration dependent manner inhibits single hTREK1 channel activity. Inhibition was quantified by estimation of the NP_o, where P_o is the channel open probability and N is the number of channels in the patch (methods). Fig. 4b and c illustrate the reduction in channel activity in terms of NP_o at 100 μM and 5 mM lidocaine respectively. The inhibition was rapid with a 50 % reduction in channel activity observed within 15.7 ± 5.1 s (n = 17) following treatment with 5 mM lidocaine. The average NP_o on application of 100 μM and 5 mM lidocaine has been illustrated as bar diagram showing the concentration dependence of hTREK1 inhibition and reversal of NP_o upon washing out lidocaine (Fig. 4d).

A decrease in channel NP_o by lidocaine could be because of an anesthetic-induced decrease in the mean open time (τ_o) and/or an increase in the mean close time (τ_c). The mean dwell times (τ_o, τ_c) were estimated by fitting the dwell time distribution histograms by mixed exponential pdfs (methods). The open time and close time distributions in our case were fitted by mono and bi-exponential functions respectively. Interestingly, the mean open time was found to be unaltered upon application of lidocaine (2.6 ± 0.8 ms for low and moderate concentrations of

Molecular Pharmacology Fast Forward. Published on July 21, 2009 as DOI: 10.1124/mol.109.056838
This article has not been copyedited and formatted. The final version may differ from this version.

lidocaine, n = 6; 100 μM in this case) as illustrated in Fig. 5a and b. However, the slow time constant of the close state ($\tau 2_{close}$) significantly increased (control: 38.4 ± 24 ms; lidocaine (100 μM): 163.6 ± 57 ms, n = 6, $p < 0.01$, Mann-Whitney test) in presence of lidocaine, whereas the fast time constant ($\tau 1_{close}$) was almost unaffected (control: 1.1 ± 0.32 ms; lidocaine: 0.89 ± 0.14 ms, n = 6; $p > 0.05$, Mann-Whitney test, Fig. 5a, b). This may explain the reduced open probability of the channel in presence of lidocaine. In addition, in presence of low concentrations of lidocaine (100 μM), there was a marked reduction in the amplitude of the unblocked open conductance levels "O" of hTREK1 (O*, O; control: -2.4 pA, -5.7 pA; 100 μM lidocaine: -2.3 pA, -2.8 pA respectively) though the unitary current amplitude remained largely unaltered, as illustrated by the amplitude histograms (Fig. 5c). At higher concentration of lidocaine (5 mM) the bursting behavior of hTREK1, observed in absence of lidocaine (Fig. 3a) was abolished, where the inhibition could be majorly attributed to the drastic reduction in open probability of single hTREK1 channels (Fig. 4c, d). However, upon washing out lidocaine, resumption of bursts and increase in the open probability, comparable to activity before application of lidocaine, could be observed (Fig. 4a and 5c).

Negative cooperativity and half-of-the-sites saturation kinetics

The observation of negative cooperativity for the inhibition of hTREK1 by lidocaine at whole-cell level (Fig. 2C) could be due to negative cooperative interaction between the individual channels in the membrane (Hehl and Neumcke, 1993) or because of the inter-subunit negative cooperativity, attributable to allosteric interaction of lidocaine with hTREK1 (Suzuki et al., 2004). In order to determine the source of negative cooperativity, we measured the response of single hTREK1 channels to a wide range of lidocaine concentrations in excised inside-out

Molecular Pharmacology Fast Forward. Published on July 21, 2009 as DOI: 10.1124/mol.109.056838
This article has not been copyedited and formatted. The final version may differ from this version.

patches. The inhibitory effect of lidocaine was found to be concentration dependent between the test range of 10 μM and 5 mM. The concentration-response data obtained from NP_o analysis was fitted to the Hill equation (see methods). The IC_{50} and the Hill coefficient were estimated to be 171 ± 23 μM and 0.56 ± 0.11 respectively (Fig. 6a), which are not significantly different from the whole-cell data shown in Fig. 2C. Hill coefficient less than 1 suggests negative cooperativity in the interaction of lidocaine with the single hTREK1 molecule. Since in excised inside-out patches, we often observed activity of only a single channel molecule, it is imperative to suggest that lidocaine induced inter-subunit negative cooperativity in the hTREK1 molecule. However, a possible existence of a cooperative interaction between individual channels could not be ruled out from our experiments.

The concentration dependent reduction in NP_o of hTREK1 was also utilized to understand the kinetics of lidocaine interaction with the channel molecule. Assuming saturating ligand concentration, the interaction of lidocaine with hTREK1 was considered to follow pseudo-first order kinetics. Pseudo-first order rate constant K_i for the inhibition of hTREK1 at a given concentration of lidocaine was determined according to the equation:

$$ln\ (NP_o/NP_o') = -K_i \times t \quad \ldots\ldots\ldots\ldots\ldots\ldots\ldots\ldots\ldots\ldots\ldots\ldots\ldots\ldots\ldots\ldots\ldots\ldots\ldots(3)$$

where NP_o' is the NP_o before lidocaine treatment and NP_o/NP_o' is the relative decrease in the NP_o after time t of lidocaine application. Fig. 6b illustrates the plot of $ln\ (NP_o/NP_o')$ against time, $t\ (min)$, the slope of which gives an estimate of the pseudo-first order rate constant $K_i\ (min^{-1})$ for a particular concentration of lidocaine (Wang and Wu, 1997). The kinetics of concentration dependent inhibition was obtained by determining the reaction order of the pseudo-first order reaction from the following equation:

$$K_i = K_i' \times [lidocaine]^n \quad \ldots\ldots\ldots\ldots\ldots\ldots\ldots\ldots\ldots\ldots\ldots\ldots\ldots\ldots\ldots\ldots(4)$$

Molecular Pharmacology Fast Forward. Published on July 21, 2009 as DOI: 10.1124/mol.109.056838
This article has not been copyedited and formatted. The final version may differ from this version.

where K_i' is the second order rate constant and *n* is the reaction order or the minimal number of lidocaine molecules involved in the interaction with the hTREK1 channel. This equation was further transformed into:

$$\log (K_i) = n \log ([lidocaine]) + \log (K_i') \quad \text{.....(5)}$$

which allows the estimation of the *n* parameter from the slope of the double logarithmic plot between K_i and concentration of lidocaine (Wang and Wu, 1997). Fig. 6c shows the double logarithmic plot, from which the reaction order was determined to be 0.47 (~0.5) for the interaction of lidocaine with hTREK1. This suggests that the interaction of lidocaine with the channel molecule is unlikely to be a simple single site binding reaction, and involves more than one allosteric site. Stoichiometrically, half reaction order (0.5) suggests that at steady state, only half of the allosteric sites on the hTREK1 molecule, which is a dimeric protein, are occupied by lidocaine. In other words, lidocaine apparently shows half-of-the-sites saturation kinetics in its interaction with hTREK1 (Fresht, 1975; Azurmendi et al., 2005). In order to verify the above findings, we compared the kinetics of lidocaine inhibition of hTREK1 with that of a known activator of the channel, 2, 2, 2- trichloroethanol (TCE), an active metabolite of the general anesthetic, chloral hydrate (Harinath and Sikdar, 2004). TCE was found to potentiate hTREK1 activity in a dose-dependent manner with an EC_{50} of 230 ± 65 μM and the Hill coefficient of 1.6 ± 0.28, suggesting strong positive cooperativity in its interaction with hTREK1. On the other hand, from similar analysis as above, we estimated the reaction order to be ~ 1.0 (0.93) (Fig. S2). Reaction order of 1 with respect to the ligand suggested a single site binding of the TCE molecule to the hTREK1 channel. This comparative kinetics highlights the basic kinetic difference between an allosteric inhibitor and an allosteric activator of the channel molecule.

Molecular Pharmacology Fast Forward. Published on July 21, 2009 as DOI: 10.1124/mol.109.056838
This article has not been copyedited and formatted. The final version may differ from this version.

C-terminal domain of hTREK1 mediates the effect of lidocaine

The positively charged quaternary ammonium analogue of lidocaine, QX314 (5 mM) was found to have no effect on the hTREK1 current at whole-cell level (n = 4; Fig. 7a). It suggests that lidocaine interacts with a domain of the hTREK1 channel that is accessible only from the intracellular side. The cytoplasmic C-terminal domain (CTD) of TREK1 has been implicated in the sensitivity of the channel to several modulators such as volatile anesthetics (Patel et al., 1999), stretch, temperature and intracellular acidosis (Maingret et al., 1999; Honore, 2007). Therefore, we evaluated the possible role of the CTD of hTREK1 in mediating the inhibitory effect of lidocaine by using C-terminal deletion mutants and single amino acid substitutions.

Deletion of the carboxy-terminal 119 residues of hTREK1 (Δ119; Fig. 7b) abolished the outward rectification property of the channel, whereas deletion of the distal 89 residues (Δ89; Fig. 7b) conferred only mild out-ward rectification (Fig. 7c). The whole-cell current density of both the deletion mutants, however, was not significantly different from the wild type hTREK1 (Fig. 7d). Interestingly, both the C-terminal deletion mutants were completely insensitive to lidocaine. Fig. 8a illustrates the comparision of the whole-cell current response of the wild-type hTREK1, Δ119 and Δ89 mutants to ramp membrane potential from -80 to 80 mV in presence of 5 mM lidocaine. The inset represents the time course of the effect of lidocaine on the whole-cell current. The percentage inhibition observed in case of wild-type (92.6 ± 5.9 %, n = 14) is significantly higher ($p < 0.001$, Mann-Whitney test) compared to Δ89 (0.56 ± 5.7 %, n = 5) and Δ119 mutants (-8.0 ± 13.9 %, n = 6) as illustrated in Fig. 8b. The effect of lidocaine (5 mM) on the mutant Δ89 and Δ119 hTREK1 channels was also investigated at single-channel level in excised inside-out patches. Fig. 8c illustrates the application of 5 mM lidocaine in an inside-out patch expressing

Molecular Pharmacology Fast Forward. Published on July 21, 2009 as DOI: 10.1124/mol.109.056838
This article has not been copyedited and formatted. The final version may differ from this version.

Δ119 mutant, which showed mild increase in single-channel activity rather than inhibition. However, the change in current amplitude, open probability and the burst behavior on application of lidocaine was insignificant. It was quantitatively expressed as the maximum open probability, NP_o of the mutant channel (Fig. 8d), which shows no significant variation upon application of lidocaine ($n = 5$, $p > 0.05$; Mann-Whitney test; Fig. 8d).

In order to map the region(s) responsible for lidocaine sensitivity in the C-terminal 89 residues, we incorporated point mutations in the CTD. The voltage-gated Na^+ channel is the known major target of local anesthetic molecules like lidocaine. Alanine scanning mutagenesis has revealed a near universal importance of two strategically placed D4/S6 aromatic residues Phe1579 and Tyr1586 (Na_v 1.4 nomenclature) in the inhibition of voltage-gated Na^+ channels by class 1A and 1B (lidocaine belongs to 1B) antiarrhythmic drugs (Ragsdale et al., 1994; Nau and Wang, 2004; Ahern et al., 2008). Further studies also attribute a cation-pi interaction to be the basis of lidocaine binding to this aromatic moiety (Ahern et al., 2008). Interestingly, we identified a sub-domain in the CTD of hTREK1 between the PKA (Protein kinase A) phosphorylation site Ser348 and PKG (cGMP-dependent kinase) phosphorylation site Ser366, having two aromatic residues Tyr352 and Phe355, ideally placed to form a local anesthetic binding site (Fig. 7b (i)). Multiple sequence alignment of the C-terminal domain of hTREK1 with the proposed local anesthetic binding region of Na_v channels from skeletal muscle (SCN4A) and the brain (SCN2A) show that the two aromatic residues Tyr352 and Phe355 along with the Ser348 residue seem to be conserved in Na_v channels (Fig. 7b (ii)) despite a weak homology at other residues in the domain. On the contrary, we found that the human TREK2 channel which shares more than 80 % homology with hTREK1 in the C-terminal domain, does not have a homologous aromatic couplet in the vicinity of the Ser residue (Fig 7b (iii)). Most surprisingly, human TREK2 has

Molecular Pharmacology Fast Forward. Published on July 21, 2009 as DOI: 10.1124/mol.109.056838
This article has not been copyedited and formatted. The final version may differ from this version.

been shown to be non-responsive to even 1 mM lidocaine (Bang et al., 2000). On the other hand, Ser348 which determines the net charge in the sub-domain depending on its phosphorylation state may affect the strength of cation-pi interaction of lidocaine. Therefore, to directly test the role of this sub-domain we utilized the following mutations: the S348A, S348D, S366A and the double mutant Y352A/F355A in the CTD. In our hands, all the above mutations yielded functional channels which largely retained the properties of hTREK1 as illustrated in Fig. 7c (and Fig. S3 for S366A). However, in case of S348A mutant the basal current level significantly increased compared to wild type hTREK1 and S348D mutation led to expression of channels, with considerably lower current density (Fig. 7c and d) as reported earlier (Murbartian et al., 2005). Though the maximum inhibition (at 5 mM lidocaine) in case of the S348A mutant (phosphorylation-defective mutant) (86.2 ± 6.4 %, n = 8) was not significantly different ($p > 0.05$, Mann-Whitney test) from the wild-type hTREK1 (92.6 ± 5.9 %, n = 14), the reversal of inhibition upon washing out lidocaine was considerably slower compared to the wild-type (Fig. 8a, inset). On the other hand, the constitutive phosphorylation mimicking mutant S348D exhibited a maximum inhibition of 41.4 ± 14.3 % (n = 5) with 5 mM lidocaine which was significantly less compared to the wild-type hTREK1 (92.6 ± 5.6, n = 14; $p < 0.01$, n = 5, Mann-Whitney test). Interestingly, the reversal of inhibition in case of S348D was comparable to the wild-type hTREK1 (Fig. 8a, inset). In order to ascertain that the minimal inhibition of the S348D mutant channel by lidocaine is not an artifact masked by the reduction in the current density, we performed experiments by activating the mutant channels (both S348A and S348D) with arachidonic acid (AA, 1 μM) prior to the application of lidocaine (5 mM). The results illustrate a similar trend in inhibition as observed without AA. S348A mutant showed a greater inhibition

Molecular Pharmacology Fast Forward. Published on July 21, 2009 as DOI: 10.1124/mol.109.056838
This article has not been copyedited and formatted. The final version may differ from this version.

whereas S348D was mildly inhibited though both of them showed marked potentiation following AA application, as illustrated in Fig. 9a.

In order to further verify the role of phosphorylation in the interaction of lidocaine with the channel, we performed experiments with the PKA activator, forskolin and inhibitor KT 5720. On application of forskolin (1μM), the hTREK1 current gradually decreased (over 3-5 minutes) and upon application of lidocaine (5 mM), there was a further mild inhibition (37.4 ± 5.3 %, n = 3) over the steady-state phosphorylated current level, as shown in Fig. 9b (i). On the other hand, incubation of cells with KT 5720 (1μM, for 10 min), PKA inhibitor, led to drastic increase in hTREK1 current with time, which was almost completely inhibited by 5 mM lidocaine (87.2 ± 4.5 % over the steady-state dephosphorylated current level, n = 3; data not shown). The reversal from inhibition, however, was gradual, similar to the phosphorylation-defective mutant, S348A (Fig. 8a). Phosphorylation of Ser348 by PKA regulates the basal level current of hTREK1 (Bockenhauer et al., 2001), as shown in our experiments. Most interestingly, the S348A mutant of hTREK1 was unaffected by forskolin (1 μM) as shown in Fig. 9b (ii), which suggests that the Ser348 indeed gets phosphorylated by PKA activity. In essence, phosphorylation at Ser348 interferes with lidocaine induced inhibition whereas dephosphorylation or incorporation of a hydrophobic residue (S348A) at the same site stabilizes the inhibited state, and delays the reversal from inhibition.

However, the S366A mutation seemed to have no effect on lidocaine mediated inhibition of hTREK1 (87 ± 5.4 %, n = 4; Fig. S3e and f). On the contrary, in case of the double mutant (Y352A/F355A), replacement of the aromatic residues with alanine drastically hampered lidocaine mediated inhibition (maximum inhibition 13.4 ± 6.0 % with 5 mM lidocaine, n = 9) as

Molecular Pharmacology Fast Forward. Published on July 21, 2009 as DOI: 10.1124/mol.109.056838
This article has not been copyedited and formatted. The final version may differ from this version.

illustrated in Fig. 8a and b. In excised inside-out patches, the double mutant behaved similar to that of the wild-type with two distinguishable open conductance levels and open channel bursts (Fig. 8e). Upon application of lidocaine (5 mM), however, there was no significant change observed compared to untreated wild-type channel (Fig. 8e). The mutant channel activity was quantified as the change in open probability (NP_o), which was not significantly different from the untreated channel activity ($n = 4$, $p > 0.05$, Mann-Whitney test; Fig. 8f). Above results suggest that the two aromatic residues Tyr352 and Phe355 are instrumental in mediating the inhibitory effect of lidocaine and phosphorylation state of the Ser348 residue plays a key role in determining the inhibitory effect of lidocaine.

Intermediate kinetics of the heterodimer of wild-type hTREK1 and Δ119 deletion mutant sheds light on the reaction mechanism

Transfection of equimolar ratio of the wt-hTREK1 and Δ119 cDNA in HEK 293 cells should result in expression of three distinct species of channels, homodimer of wild-type $hTREK1_{wt}$, homodimer of Δ119 and heterodimer of wt-hTREK1 and Δ119 (Czirjak and Enyedi, 2002). Consistent with this, we observed three different populations of channels constituting the whole-cell current obtained from HEK 293 cells transfected with wt-hTREK1 and Δ119 cDNA. The whole-cell current profile from such cells was intermediate between that of wt-hTREK1 and Δ119 homodimer expressing cells. The whole-cell current was mildly outwardly rectifying as illustrated in Fig. S3a and b. The time-dependent component of the whole-cell current was estimated from the ratio of the steady-state current (I_{st}) to the current at time 0 (I_0) (Maingret et al., 2002). Cells expressing both the wt-hTREK1 and Δ119 exhibited intermediate time-dependency ($I_{st}/ I_0 = 1.4 \pm 0.2$ compared to 1.95 ± 0.12 for wt-hTREK1 and 1.1 ± 0.1 for Δ119, n

Molecular Pharmacology Fast Forward. Published on July 21, 2009 as DOI: 10.1124/mol.109.056838
This article has not been copyedited and formatted. The final version may differ from this version.

= 4; Fig. S3c). The three populations became more apparent on application of lidocaine by virtue of their differential response to lidocaine. Fig. 10a illustrates the time course of the whole-cell current response of cells expressing wt-hTREK1, Δ119 alone and cells expressing both of them. The maximum steady-state inhibition observed in cells expressing the heterodimer $hTREK1_{wt}$-Δ119 was 54.8 ± 9.9 (n = 6), which is intermediate between wt-hTREK1 (92.6 ± 5.9 %, n = 8) and Δ119 mutant (-8.0 ± 13.9 %, n = 5) as illustrated in Fig. 10d. The inhibition time course (Fig. 10a) was fitted with exponential functions (methods) to obtain the mean decay times. In case of wild-type hTREK1, the decay could be fitted to a single exponential with time constant 18.8 ± 5.0 s (n = 6), whereas in cells expressing $hTREK1_{wt}$-Δ119, the decay had two exponential components with time constants, $\tau 1$ = 16.6 ± 12.6 s and $\tau 2$ = 170.2 ± 65.4 s (n = 4; Fig. 10b). The fast inhibition corresponds to the wt-hTREK1; the uninhibited component corresponds to the population of Δ119 mutant, whereas the slower inhibition is presumably due to the population of heterodimers of wt-hTREK1 and Δ119. This was further supported by excised inside-out single-channel recordings from cells expressing both wt-hTREK1 and Δ119. We observed 3 distinct classes of single-channel activities which exhibited different sensitivities to lidocaine (5 mM) as illustrated in Fig. 10c. They were distinguished by the percentage reduction in their open probability (NP_o) (Fig. 10e). The channels with intermediate sensitivity to lidocaine (% reduction in NP_o = 51.6 ± 10.5, 3 out of 11 patches) was significantly different from channels with high sensitivity to lidocaine (% reduction in NP_o = 87 ± 8.2; 5 out of 11 patches) and those which are insensitive to lidocaine (% reduction in NP_o = -2.6 ± 12.3, 3 out of 11 patches). These channels represent the population of heterodimers of wt-hTREK1 and Δ119. These results suggest that co-expression of wt-hTREK1 and Δ119 leads to expression of a distinct population of heterodimers

Molecular Pharmacology Fast Forward. Published on July 21, 2009 as DOI: 10.1124/mol.109.056838
This article has not been copyedited and formatted. The final version may differ from this version.

which exhibit partial inhibition upon lidocaine treatment. It further highlights the fact that the C-terminal domain is essential for lidocaine mediated inhibition, but a single C-terminal domain is not sufficient for maximum inhibition observed in case of wt hTREK1.

Molecular Pharmacology Fast Forward. Published on July 21, 2009 as DOI: 10.1124/mol.109.056838
This article has not been copyedited and formatted. The final version may differ from this version.

Discussion

The present study investigated the inhibitory action of lidocaine on the human K_{2P} channel, TREK1. We report here a unique aromatic couplet (Tyr-Phe) in the vicinity of the PKA phosphorylation site in the CTD of hTREK1, which is critical for the action of lidocaine on hTREK1. Furthermore, we elucidate a novel kinetic paradigm, involving inter-subunit negative cooperativity and half-of-the-sites saturation of the allosteric sites, for this class of amide local anesthetics.

Inhibition of hTREK1 by lidocaine: role of phosphorylation and the aromatic couplet in the CTD

Lidocaine inhibited the hTREK1 channel reversibly and in a dose-dependent manner, both at whole-cell and single-channel level (IC_{50} of ~180 μM; Fig. 2c and 6a). In physiological condition, whole-cell hTREK1 current exhibited a leak or instantaneous component and a time-dependent component owing to the differential distribution of channels between two functionally distinct closed states C_1 and C_2 (Kennard et al., 2005). The instantaneous component of the whole-cell current represents channels in C_2 moving to the single open state O, while the time-dependent component represents channels moving more slowly from the resting close state C_1 to O. Since lidocaine inhibits both the components of the whole-cell current (Fig. 2f), we propose that lidocaine binds non-specifically to both the close states of the channel. On the other hand, at single-channel level, the mean close time ($\tau 2$) for the long closures increased significantly (Fig. 5b) in presence of lidocaine whereas the mean open time and the unitary current amplitude of hTREK1 were unaffected (Fig. 5a, c). The increase in the mean close time owes to the appearance of more frequent long close events upon treatment with lidocaine. The frequency and duration of long-lived close state depend on the stabilization of the close state and have been

Molecular Pharmacology Fast Forward. Published on July 21, 2009 as DOI: 10.1124/mol.109.056838
This article has not been copyedited and formatted. The final version may differ from this version.

implicated in the regulation of gating of the leak K^+ channels (Zilberberg et al., 2001; Ben-Abu et al., 2009). Above evidences suggests that lidocaine stabilizes the close state to manifest its inhibitory action on the channel.

Modulation of single-channel kinetic properties by lidocaine in excised inside-out patches and our work with the permanently charged analogue of lidocaine, QX314 (Fig. 7a) suggested that lidocaine interacts with the channel from the intracellular side. Further, our studies with the deletion mutants revealed that the inhibitory effect of lidocaine was completely abolished in the C-terminal deletion mutants of hTREK1 (Δ89 and Δ119, Fig. 8) underlining the importance of the CTD in mediating the effect of lidocaine. On further analysis of the CTD, we identified two strategically placed unique aromatic residues Tyr352 and Phe355 in the vicinity of the PKA phosphorylation site Ser348 which were analogous to the aromatic couplet implicated in the interaction of lidocaine with voltage-gated Na^+ channels (Ragsdale et al., 1994; Nau and Wang, 2004, Ahern et al., 2008). Interestingly, the double alanine-substitution mutant of the aromatic couple (Y352A/F355A) abolished the inhibitory effect of lidocaine on hTREK1, both at whole-cell and single-channel level (Fig. 8 b, f), analogous to the finding in Na_v channels. Surprisingly, hTREK2 which is insensitive to high concentration of lidocaine (Bang et al., 2000) lacks the two aromatic residues despite sharing high homology with the hTREK1 CTD (Fig. 7b (iii)). Thus, this aromatic couplet might be an indispensable component of the lidocaine binding site in hTREK1. Further evidence in favor of a distinct lidocaine binding site came from the mutagenesis studies of the PKA phosphorylation site Ser348, which suggests that the presence of a charged moiety at this site reduces the inhibitory effect of lidocaine by destabilizing the inhibitory complex. In essence, the sub-domain encompassing Ser348 to Phe355 is critical for the interaction of lidocaine with hTREK1 where the phosphorylation state of Ser348, in

conjunction with the aromatic couplet, determine the binding efficacy of lidocaine. Since the presented results are from an isoform of hTREK1 with an intact NTD and as the N-terminus is not involved in mediating the effect of anesthetics (Patel et al., 1999) and other ligands (Thomas et al., 2008), we conclude that the inhibitory effect of lidocaine is mediated by the CTD of hTREK1 independent of the NTD. Moreover, the ability of lidocaine to affect channel gating by binding to a site in the CTD qualifies it as an allosteric inhibitor of the hTREK1 channel.

Inter-subunit negative cooperativity and half-of-sites saturation binding kinetics

From the concentration-response curve of lidocaine binding to hTREK1, we estimated the Hill coefficient to be 0.49 (< 1), which suggests that the interaction of lidocaine with the channel is strongly negatively cooperative. Negative cooperativity in case of ion channels is a fairly common phenomenon in allosteric antagonism and has been attributed to interaction between individual ion channels (K_{ATP}, Hehl and Neumcke, 1993), identical monomers (metabotropic GluR, Suzuki et al., 2004) and independent binding sites on the channel having different affinities for the ligand (connexin40 gap junction channels, Lin and Veenstra, 2007). We observed strong negative cooperativity in the interaction of lidocaine with single hTREK1 channel in excised inside-out patches (Fig. 6a), which largely eliminates the possibility of any allosteric interaction among individual channels. TREK1 is a homodimeric protein with two identical CTD, which serve as the docking sites for lidocaine. Since the CTD deletion and the Y352A/F355A double mutant of hTREK1 were predominantly insensitive to lidocaine, we rule out the possibility of other allosteric sites having differential affinities for lidocaine. Therefore, we conclude that lidocaine induced negative cooperativity is the result of inter-subunit interaction within the hTREK1 molecule.

Molecular Pharmacology Fast Forward. Published on July 21, 2009 as DOI: 10.1124/mol.109.056838
This article has not been copyedited and formatted. The final version may differ from this version.

A limiting case of negative cooperativity, where only half of the allosteric binding sites are occupied by ligands, has been described as the "half-of-the-sites binding stoichiometry" and has been known to facilitate the inhibitory action of antagonists (Fresht, 1975). Our finding of half reaction order (0.47) with respect to lidocaine in the pseudo-first order reaction involving lidocaine and the channel (Fig. 6c), suggested that only one molecule of lidocaine binds to hTREK1 homodimer despite the availability of two structurally identical CTD. In other words, the reaction followed the half-of-the-sites saturation binding kinetics. Our studies with the heterodimer hTREK1$_{wt}$-Δ119 illustrated that the single CTD of the heterodimer is capable of mediating partial inhibition by lidocaine, but for complete inhibition both the intact CTD are essential (Fig. 10). It further emphasizes the fact that each of the CTD of hTREK1 is an independent binding site of lidocaine but complete inhibition necessitates the cooperative interaction between both the CTDs upon lidocaine binding. In contrast, TCE binding to the channel molecule seemed to be a simple single site binding (reaction order with respect to TCE was ~ 1.0; Fig. S2), which confirms that the half-of-the-sites binding stoichiometry is specific to the interaction of lidocaine and the CTDs of hTREK1.

A model explaining the simultaneous observation of negative cooperativity and half-of-the-sites saturation kinetics

Both negative cooperativity and half-of-the-sites binding stoichiometry are generally accompanied by ligand-induced structural asymmetry in multi-subunit proteins (Azurmendi et al., 2005). To explain the above two phenomena in lidocaine interaction with hTREK1, we propose a kinetic model, adapted from the studies of the enzyme tyrosyl-tRNA-synthetase (Fresht, 1975). We propose that binding of two lidocaine molecules one to each of the identical

Molecular Pharmacology Fast Forward. Published on July 21, 2009 as DOI: 10.1124/mol.109.056838
This article has not been copyedited and formatted. The final version may differ from this version.

CTD would probably result in steric clash in the transient two lidocaine molecules plus channel complex as shown in Fig. 11a (i), which immediately disintegrates to give rise to a more stable hTREK1-lidocaine inhibitory complex having only one lidocaine bound to the channel (Fig. 11a (ii)). In the kinetic model presented in Fig. 11b, *k2* is the apparent rate constant for formation of the transient partial inhibitory complex ($[T.L]_i$), and *k1' << k2' and k2''* as the binding of second lidocaine molecule to TREK1 is highly unfavorable. This explains the rapid formation of the stable inhibitory complex containing only one lidocaine, shown in Fig. 11b (Fresht, 1975). The present model is only descriptive in nature where the rate constants involved in the kinetic scheme have not been estimated. However, it satisfactorily explains both the negative cooperativity and the half reaction order observed in our case. Results with the hTREK1 heterodimer ($hTREK1_{wt}$-Δ119, Fig. 10) suggests the existence of the partial inhibitory complex ($[T.L]_i$). Nevertheless, negative cooperativity has an important physiological implication in extending the lidocaine concentration range to which the hTREK1 molecule responds such that substantial amount of inhibition can be observed even at very low concentrations of lidocaine (Suzuki et al., 2004).

In various clinical settings, the plasma concentration of lidocaine can range from 20-30 μM to as high as 10 mM (Johnson et al., 2004). Since, we observed significant block of hTREK1 even at very low concentrations of lidocaine (10 μM), TREK1 block might have important clinical consequences. Moreover, inhibition of leak K^+ channels increases membrane excitability (Drachman and Strichartz, 1991), which could explain the adverse neurological symptoms (Benkwitz et al., 2003) of lidocaine.

Molecular Pharmacology Fast Forward. Published on July 21, 2009 as DOI: 10.1124/mol.109.056838
This article has not been copyedited and formatted. The final version may differ from this version.

Acknowledgements: We are grateful to Prof. Steve A.N. Goldstein, Yale University medical school for providing the clone and the S348A mutant of hTREK1 and Prof. Bert Vogelstein, John Hopkins Oncology Centre for the AdEasy1 system. We are also thankful to S. Chatterjee for her help in some of the molecular biology experiments.

Molecular Pharmacology Fast Forward. Published on July 21, 2009 as DOI: 10.1124/mol.109.056838
This article has not been copyedited and formatted. The final version may differ from this version.

References

Ahern CA, Eastwood AL, Dougherty DA, Horn R (2008) Electrostatic contributions of aromatic residues in the local anesthetic receptor of voltage-gated sodium channel. *Circ Res* **102**: 86-94

Azurmendi HF, Miller SG, Whitman CP, Mildvan AS (2005) Half-of-the-sites binding of reactive intermediates and their analogues to 4-oxalocrotonate tautomerase and induced structural asymmetry of the enzyme. *Biochemistry* **44**: 7725-7737.

Bang H, Kim Y, Kim D (2000) TREK 2, a new member of the mechanosensitive tandem pore K^+ channel family. *J Biol Chem* **275**: 17412-17419

Ben-Abu Y, Zhou Y, Zilberberg N, Yifrach O (2009) Inverse coupling in leak and voltage-activated K^+ channel gates underlies distinct roles in electrical signaling. *Nat Str Mol Biol* **16**: 71-79.

Benkwitz C, Garrison J, Linden J, Durieux M, Hollman M (2003) Lidocaine enhances $G_{\alpha i}$ protein function. *Anesthesiology* **99**: 1093-1101.

Bockenhauer D, Zilberberg N, Goldstein SAN (2001) KCNK2: reversible conversion of a hippocampal potassium leak into a voltage-dependent channel. *Nat Neurosci* **4**: 486-491.

Carmeliet E, Morad M, Vander HG, Vereecke J (1986) Electrophysiological effects of tetracaine in single guinea-pig ventricular myocytes. *J Physiol* **376**: 143-161.

Colquhoun D, Sigworth FJ (1983) Fitting and statistical analysis of single-channel records. In: *Single-Channel Recording* (Sackmann B, and Neher E eds) pp 191-264, Plenum Press: New York.

Cuevas J, Adams DJ (1994) Local anesthetic blockade of neuronal nicotinic acetylcholine receptor channels in rat parasympathetic ganglion cells. *Br J Pharmacol* **111**: 663-672.

Czirjak G, Enyedi P (2002) Formation of functional heterodimers between TASK1 and TASK3 two-pore domain potassium channel subunits. *J Biol Chem* **277**: 5426-5432.

DeToledo JC (2000). Lidocaine and seizures. *Ther Drug Monit* **22**:320–322

Drachman D, Strichartz G (1991) Potassium channel blockers potentiate impulse inhibition by local anesthetics. *Anesthesiology* **75**: 1051-1061.

Fresht AR (1975) Demonstration of two active sites on a monomeric aminoacyl-tRNA synthetase: possible roles of negative cooperativity and half-of-the-sites reactivity in oligomeric enzymes. *Biochemistry* **14**: 5-12.

Gonzalez T, Longobardo M, Caballero R, Delpon E, Tamargo J, Valenzuela C (2001) Effects of bupivacaine and a novel local anesthetic, IQB-9302, on human cardiac K^+ channels. *J Pharmacol Exp Ther* **296**: 573-583.

Hamill OP, Neher E, Sackman B, Sigworth FJ (1981) Improved Patch-clamp techniques for high-resolution current recording from cells and cell-free membrane patches. *Pflugers Arch* **391**: 85-100.

Harinath S, Sikdar SK (2004) Trichloroethanol enhances the activity of recombinant TREK1 and TRAAK channels. *Neuropharmacol* **46**: 750-760.

He T-C, Zhou S, Costa LT, Yu J, Kinzler KW, Vogelstein B (1998) A simplified system for generating recombinant adenoviruses. *Proc Natl Acad Sci* **95**: 2509-2514.

Hehl S, Neumcke B (1993) Negative cooperativity may explain flat concentration response curves of ATP-sensitive potassium channels. *Eur Biophys J* **22**: 1-4.

Honore E (2007) The neuronal background K_{2P} channels: focus on TREK1. *Nat rev Neurosci* **8**: 251-261.

Johnson ME, Uhl CB, Spittler K, Wang H, Gores GJ (2004) Mitochondrial injury and caspase activation by the local anesthetics lidocaine. *Anesthesiology* **101**: 1184-1194.

Kennard LE, Chumbley JR, Ranatunga KM, Armstrong SJ, Veale EL, Mathie A (2005) Inhibition of the human two-pore domain potassium channel, TREK1, by fluoxetin and its metabolite norfluoxetine. *Br J Pharmacol* **144**: 821-829.

Kindler CH, Paul M, Zou H, Liu C, Winegar BD, Gray AT et al (2003) Amide local anesthetics potently inhibit the human tandem pore domain background K^+ channel TASK2 (KCNK5). *J Pharmacol Exp Ther* **306**: 84-92.

Kindler CH, Yost CS (2005) Two-pore domain potassium channels: new sites of local anesthetics action and toxicity. *Reg anesth pain med* **30**: 260-274.

Komai H, McDowell TS (2001) Local anesthetic inhibition of voltage-activated potassium currents in rat dorsal root ganglion neurons. *Anesthesiology* **94**:1089-1095.

Lesage F, Guillemare E, Fink M, Duprat F, Lazdunski M, Romey G et al (1996) TWIK-1, a ubiquitous human weakly inward rectifying K^+ channel with a novel structure. *EMBO J* **15**: 1004-1011.

Lin X, Veenstra RD (2007) Effect of transjunctional KCl gradients on the spermine inhibition of Connexin40 gap junctions. *Biophys J* **93**: 483-495.

Maingret F, Patel AJ, Lesage F, Lazdunski M, Honore E (1999) Mechano- or acid stimulation, two interactive modes of activation of TREK1 potassium channel. *J Biol Chem* **274**: 266691-26696.

Maingret F, Honore E, Lazdunski M, Patel AJ (2002) Molecular basis of voltage-dependent gating of TREK1, a mechano-sensitive K^+ channel. *Biochem Biophys Res Comm* **292**: 339-346

Murbartian J, Lei Q, Sando JJ, Bayliss DA (2005) Sequential phosphorylation mediates receptor and kinase-induced inhibition of TREK1 background potassium channels. *J Biol Chem* **280**: 30175-30184.

Nau C, Wang GK (2004) Interaction of local anesthetics with the voltage-gated Na^+ channels. *J Membr Biol* **201**: 1-8.

Ness TJ (2000) Intravenous lidocaine inhibits visceral nociceptive reflexes and spinal neurons in the rat. *Anesthesiology* **92**: 1685-1691.

Nishizawa N, Shirasaki T, Nakao S, Matsuda H, Shingu K (2002) The inhibition of the N-methyl-D-Aspartate receptor channel by local anesthetics in mouse CA1 pyramidal neurons. *Anesth Analg* **94**: 325-330.

Patel AJ, Honore E, Lesage F, Fink M, Romey G, Lazdunski M (1999) Inhalation anesthetics activate two-pore-domain background K^+ channels. *Nat Neurosci* **2**: 422-426.

Punke MA, Licher T, Pongs O, Friederich P (2003) Inhibition of human TREK1 channels by bupivacaine. *Anesth Analg* **96**:1665-1673.

Ragsdale DS, McPhee JC, Scheuer T, Catterall WA (1994) Molecular determinants of state dependent block of Na^+ channels by local anesthetics. *Science* **265**: 1724-1728.

Simkin D, Cavanaugh EJ, Kim D (2008) Control of the single channel conductance of K_{2P}10.1 (TREK2) by amino-terminus: role of alternative translation initiation. *J Physiol* **586**: 5651-5663

Suzuki Y, Moriyoshi E, Tsuchiya D, Jingami H (2004) Negative cooperativity of glutamate binding in the dimeric metabotropic glutamate receptor subtype 1. *J Biol Chem* **279**: 35526-35534.

Thomas D, Plant LD, Wilkens CM, McCrossan ZA, Goldstein SAN (2008) Alternative translation initiation in rat brain yields K_{2P}2.1 potassium channel permeable to sodium. *Neuron* **58**: 859-870.

Wang R, Wu L (1997) The chemical modification of K_{Ca} channels by carbon monoxide in vascular smooth muscle cells. *J Biol Chem* **272**: 8222-8226.

Zilberberg N, Ilan N, Goldstein SAN (2001) KCNKØ: Opening and closing the 2-P-domain potassium leak channel entails "C-type" gating of the outer pore. *Neuron* **32**: 635-648.

Zhou W, Arrabit C, Choe S, Slesinger PA (2001) Mechanism underlying bupivacaine inhibition of G-protein gated inwardly rectifying K^+ channels. *Proc Natl Acad Sci* **98**: 6482-6487.

Molecular Pharmacology Fast Forward. Published on July 21, 2009 as DOI: 10.1124/mol.109.056838
This article has not been copyedited and formatted. The final version may differ from this version.

Footnotes

The research was supported by grants from the Department of Science and Technology (DST), Govt. of India. TKN was supported by the Senior Research fellowship from Council of Scientific and Industrial Research (CSIR), India.

§ Address correspondence to: S.K. Sikdar, Molecular Biophysics Unit, Indian Inst. of Science, Bangalore-560012. E-mail: sks@mbu.iisc.ernet.in.

Legends for figures

Fig 1 mRNA expression of hTREK1 in Ad-hTREK1 infected HEK 293 cells a. SYBR Green real-time PCR kinetic data traces for the genes hTREK1 and β-Actin. Open symbols: cDNA from cells (Ad-GFP and Ad-hTREK1 infected) amplified with hTREK1 specific primer; closed symbols: cDNA from cells amplified with β-actin specific primer. b. Corresponding melting or dissociation curves of the real-time PCR products for the same reaction as in a. c. The specific amplification of hTREK1 in Ad-hTREK1 infected cells illustrated by 0.4 Kb amplicon of hTREK1 gene (marked by arrow). Lanes: 1. 100 bp marker 2, 5. cDNA from uninfected HEK 293 cells. 3, 6. cDNA from cells infected with AdGFP. 4, 7. cDNA from cells infected with Ad-hTREK1. d. Fold increase in the hTREK1 mRNA expression in Ad-hTREK1 infected HEK 293 cells as quantified from real-time PCR data.

Fig 2 Lidocaine inhibits whole-cell hTREK1 channel current a. hTREK1 current evoked by ramp changes in voltage (-100 to 100 mV) in control condition and in presence of increasing concentrations of lidocaine. The holding potential was -80 mV and the test concentrations have been illustrated in the figure. b. Inhibition of hTREK1 current was reversible on washing out even high concentration of lidocaine (5 mM) illustrated by raw current traces elicited by ramp voltage pulses as in a. c. Concentration-response curve for lidocaine inhibition of hTREK1 current. Numbers above the data points correspond to the number of cells tested for each concentration of lidocaine. d. Current-clamp recordings of membrane potential of HEK 293 cells infected with Ad-hTREK1 under control condition, during application of 0.5 mM lidocaine and following washout of the drug. Note the membrane depolarization and reversibility of the membrane potential upon washing out of lidocaine. e. Lidocaine non-specifically inhibits both the instantaneous (highlighted by asterisk) and time- dependent component (pointed by arrow) of

Molecular Pharmacology Fast Forward. Published on July 21, 2009 as DOI: 10.1124/mol.109.056838
This article has not been copyedited and formatted. The final version may differ from this version.

whole-cell hTREK1 current (gray lines). Whole-cell current was evoked by rectangular 50 ms voltage pulse from -80 mV to 40 mV in absence (control) and presence of 1 mM lidocaine. The black curves superimposing the current traces represent the exponential function fitted to the activation time course. f. Percentage inhibition of the time-dependent (TD) and non-time-dependent (NTD) components of hTREK1 current in presence of 1 mM lidocaine (*: $p < 0.05$). g. Lidocaine induced inhibition was independent of voltage. Voltage-dependent inhibition was analyzed by comparing percentage inhibition in whole-cell steady-state current amplitudes at three different membrane potentials: -40, 0, and 40 mV, respectively in presence of 0.1 mM lidocaine. The difference in inhibition was not significant (n.s).

Fig 3 Characterization of single hTREK1 channels in excised inside-out patches a.(i) A single hTREK1 channel at varying membrane potentials (as indicated) in symmetrical K^+ gradient showing reversal at 0 mV. Shown here are the two open conductances O* (blocked, -2.9 pA) and O (unblocked, 6.8 pA) at hyperpolarized potential (-60 mV) owing to the internal Mg^{2+} block. Note the mild outward rectification of single hTREK1 channel. (ii) Part of the trace at -60 mV, illustrated at high resolution. Note the presence of the two open conductance levels depicted by dotted lines. The arrow points to the flickery short duration close state within the burst and the asterisk marks the long inter-burst close state. b. Single hTREK1 channel current evoked in symmetrical K^+ gradient by a ramp pulse depicted below the current tracing. c. Single channel current-voltage relationship obtained by measuring the unitary current amplitudes at varying potentials in symmetric and physiological K^+ gradients. The reversal potential of hTREK1 shifted from -84 mV to 0 mV on changing the external K^+. The measured slope conductance was 95.7 ± 9.4 pS (n = 7). d. TREK1 is a mechano-gated channel. Note the prominent increase in open probability of hTREK1 on application of negative pressure through the patch pipette.

Molecular Pharmacology Fast Forward. Published on July 21, 2009 as DOI: 10.1124/mol.109.056838
This article has not been copyedited and formatted. The final version may differ from this version.

Fig 4 Inhibition of single-channel hTREK1 current by lidocaine a (i) Single-channel current recordings obtained at -60 mV in excised inside-out configuration under control condition, during application of lidocaine [100 μM (upper panel) and 5 mM (lower panel)] and after wash out. Note the concentration dependent reduction in open probability and absence of burst behavior of the channel upon application of lidocaine. (ii) Part of the traces highlighted by dotted boxes in (i) has been illustrated at higher time resolution. b. Plot of hTREK1 open probability (NP_o) from an excised inside-out patch in control condition, in presence of 100 μM lidocaine and upon wash out. The averaged NP_o was sampled every 5 s and plotted versus time (s). The horizontal bar represents the duration for which lidocaine was applied. c. Plot of hTREK1 NP_o from the same patch as above under control condition, in presence of 5 mM lidocaine and upon wash out. The averaged NP_o was sampled and plotted versus time (s) as in b. The horizontal bar represents the duration for which lidocaine was applied. d. Comparision of average open probability (NP_o) of hTREK1 from the data in b and c in control condition, in presence of lidocaine and upon wash out. The concentrations of lidocaine used, are indicated in the figure.

Fig 5 Explanation for lidocaine induced inhibition of hTREK1 current from single-channel analysis a. Dwell time distribution histograms for the open and close times in case of control (upper panel) and in presence of 100 μM lidocaine (lower panel) obtained from patches containing only one channel. The solid curves represent the probability density functions fitted to the histograms. b. Comparision of mean dwell times (τ in ms) in case of control (C) and in presence of 100 μM lidocaine (L) (**: $p < 0.01$). c. Single-channel current evoked in control condition (upper panel), in presence of 100 μM lidocaine (middle) and following wash out (lower panel) along with the corresponding amplitude histograms. Illustrated here are the

Molecular Pharmacology Fast Forward. Published on July 21, 2009 as DOI: 10.1124/mol.109.056838
This article has not been copyedited and formatted. The final version may differ from this version.

conductance levels C (close), O (open) and O* (horizontal bars in the current tracings) and the corresponding humps in the amplitude histograms. Note the reduction in current amplitude of the unblocked open level (raw data as well as amplitude histogram) upon lidocaine application though the unitary current remains unaltered.

Fig 6 Concentration response and kinetic analysis of lidocaine binding to hTREK1 a. The concentration response curve of lidocaine inhibition fitted to the Hill's equation (see method). The estimated Hill's coefficient was 0.57 (< 1) suggesting negative cooperativity. Note the mild concavity in the log-linear plot, which is a signature of negative cooperativity. Numbers above the graph correspond to the number of cells tested for each concentration of lidocaine. b. Lidocaine induced decrease in NP_o of hTREK1 channel as a function of time. Each data point represents the mean NP_o during 30 s (0.5 min) recording periods. Pseudo-first order rate constants K_i (min^{-1}) for the inhibition were determined from the slope of the plot as described in the text (see results). c. Double logarithmic plot between the pseudo-first order rate constant K_i (min^{-1}) and concentration of lidocaine for determining the kinetic order of the reaction between lidocaine and the hTREK1. The slope of the double-logarithmic plot gives an estimate of the order of the reaction with respect to lidocaine.

Fig 7 Mapping of the lidocaine binding site in the c-terminal domain of hTREK1 a. QX314 (5 mM), a positively charged quaternary lidocaine derivative has no effect on hTREK1 currents. Whole-cell current evoked from a holding potential of -80 mV by a voltage ramp from -100 to 60 mV. The difference in current with and without QX314 at 60 mV was insignificant ($p > 0.05$, n = 4, Mann-Whitney test). b. (i) Cartoon representation of the C-terminal domain of hTREK1illustrating the deletions and point mutations. The amino acid residues at the beginning

Molecular Pharmacology Fast Forward. Published on July 21, 2009 as DOI: 10.1124/mol.109.056838
This article has not been copyedited and formatted. The final version may differ from this version.

of deletions (G and A), the phosphorylation sites (S) and the aromatic couplet (Y and F) are indicated. (ii) Multiple sequence alignment of the domain of CTD encompassing S348, Y352 and F355 with the proposed lidocaine binding domain of SCN4A and SCN2A from various origins. The highlighted regions represent the conserved residues. (iii) Pairwise alignment of the CTD of hTREK1 and hTREK2. The asterisk (*) represents the identical residues in the sequence, whereas the arrows indicate the absence of the residues Y and F in the hTREK2 CTD. c. Whole-cell current profiles of wt-hTREK1 and mutant hTREK1 channels. Note the difference in the rectification properties and maximum steady state current amplitudes (different y-scale bars) of the wt-hTREK1 and mutant channels. The whole-cell current was elicited by step pulses (-100 mV to 60 mV) from a holding potential of -80 mV. d. Comparision of whole-cell current densities (pA/pF) of hTREK1 and mutants of hTREK1 expressing HEK 293 with that of untransfected HEK 293 (wt). The numbers on the bars depict the number of cells tested.

Fig 8 Analysis of the C-terminal domain mutants reveal the binding site for lidocaine a. Whole-cell current recorded from HEK 293 cells expressing wt-TREK1, C-terminal deletion mutants Δ119 and Δ89 hTREK1, point mutants S348A and S348D and the double mutant Y352A/F355A of hTREK1 by application of voltage ramp from -80 mV to 80 mV. a: the steady state current before application of lidocaine; b: the steady state current after application of 5 mM lidocaine; c: current after wash-out of lidocaine. Inset represents the time course of inhibition of whole-cell current (normalized) by lidocaine. a, b, and c on the time course represent the time points where the whole-cell currents were sampled and displayed. X- axis scale bar of the inset: 100 s and the horizontal bars above the time-course represent the duration of lidocaine application. b. Percentage inhibition of the whole-cell current upon application of lidocaine (5 mM) expressed as mean ± SEM. The numbers represent the number of cells tested. c. (i) Single-channel current

traces recorded in inside-out configuration from a patch containing C-terminal deletion mutant Δ119 hTREK1 at -60 mV in control, during application of 5 mM lidocaine and following wash out. Note that the single-channel current remains unchanged in presence of high concentration of lidocaine. (ii) Part of the trace in (i) has been illustrated in high resolution. Note the difference in time scale. d. Comparision of average NP_o observed in control and in presence of 5 mM lidocaine. Data presented as mean ± SEM; n.s: not significant. e. (i) Single-channel current traces recorded in inside-out patch expressing the double mutant Y352A/F355A as above. (ii) Part of the trace in (i) has been illustrated in high resolution as above. Single-channel current was virtually unaffected in case of the mutant. f. Comparison of average NP_o observed in control and in presence of 5 mM lidocaine on this patch. Data presented as mean ± SEM; n.s: not significant.

Fig 9 Effect of lidocaine on hTREK1 (wt and mutant) following activation by arachidonic acid and forskolin (PKA activator). a. Whole-cell current recorded from HEK 293 cells expressing the phosphorylation-defective mutant S348A (i) and the constitutive phosphorylation mutant S348D (ii) by application of voltage ramp from -80 mV to 60 mV. In both cases, a: the current before application of lidocaine; b: the current after application of 1 μM arachidonic acid; c: current after application of 5 mM lidocaine. Inset in both (i) and (ii) represents the time course of inhibition of whole-cell current (at + 40 mV) by lidocaine. a, b, and c on the time course represent the time points where the whole-cell currents by applying voltage ramps were sampled and displayed. b. Whole-cell current recorded from HEK 293 cells expressing wt-hTREK1 (i) and the phosphorylation-deficient mutant of hTREK1, S348A (ii) by application of voltage ramp from -80 mV to 60 mV on application of lidocaine followed by PKA activator, forskolin. In both (i) and (ii), a: the current before application of forskolin; b: the current after application of 1 μM

forskolin; c: current after application of 5 mM lidocaine following application of forskolin; d: current after washing out both lidocaine and forskolin. Inset in both (i) and (ii) represents the time course of inhibition. a, b, c and d on the time course represent the time points where the whole-cell currents to voltage ramps were sampled and displayed.

Fig 10 Kinetics of the heterodimer of wt-hTREK1 and Δ119 mutant. a. The typical time course of the whole-cell response (normalized) of cells expressing hTREK1, Δ119 hTREK1 and equimolar ratio of both cDNA ($hTREK1_{wt}$- Δ119). Note the intermediate response of $hTREK1_{wt}$ - Δ119 cells. The horizontal bar represents the duration of lidocaine (5 mM) application. b. The mean decay times (τ) obtained from the exponential fits of the inhibition time course (a) of hTREK1 and $hTREK1_{wt}$ - Δ119 cells. **: $p < 0.01$. c. Single-channel response from patches expressing the homodimer hTREK1, Δ119 hTREK1 and heterodimer $hTREK1_{wt}$ - Δ119 in control condition (upper panel) and following application of 5 mM lidocaine (lower panel). Note the drastic reduction in open events in case of hTREK1, and the moderate effect of lidocaine on the heterodimer, whereas the Δ119 CTD mutant seemed to be insensitive to lidocaine. Also note that the unblocked open state 'o' is absent in the homodimer Δ119 mutant but is rescued in the heterodimer. d. Percentage inhibition of whole-cell current obtained from cells in a, presented as mean ± SEM. The numbers on the bars represent the cells tested. e. Percentage inhibition of the maximum open probability (*NPo*) obtained from patches in c, presented as mean ± SEM. The numbers on the bars represent the cells tested.

Fig 11 Model explains the inhibition of hTREK1 by lidocaine a. The schematic representation of lidocaine binding to hTREK1 (i) Model of hTREK1 bound to two molecules of lidocaine at the CTDs. Note the strong steric inhibition for the binding of the second lidocaine molecule due to

Molecular Pharmacology Fast Forward. Published on July 21, 2009 as DOI: 10.1124/mol.109.056838
This article has not been copyedited and formatted. The final version may differ from this version.

negative cooperativity. (ii) Model illustrating the stable inhibitory complex of hTREK1 and one molecule of lidocaine after the second lidocaine uncouples from the unstable complex in (i) leading to half-of-the-sites saturation kinetics. b. Kinetic model explaining both negative cooperativity and half reaction order or half-of-the-sites reaction stoichiometry. In the reaction scheme for the inhibition of hTREK1 by lidocaine T: hTREK1, *ki*: transition rate constants, T.L: Single lidocaine molecule bound to hTREK1, T.L.L*: Complex of two lidocaine bound to hTREK1, $[T\text{-}L]_i$: Partial inhibitory complex with single lidocaine molecule bound to one of the CTDs, $[T\text{-}L]_I$' or $[T\text{-}L^*]_I$': Lidocaine bound hTREK1 complete and stable inhibitory complex.

Fig 1

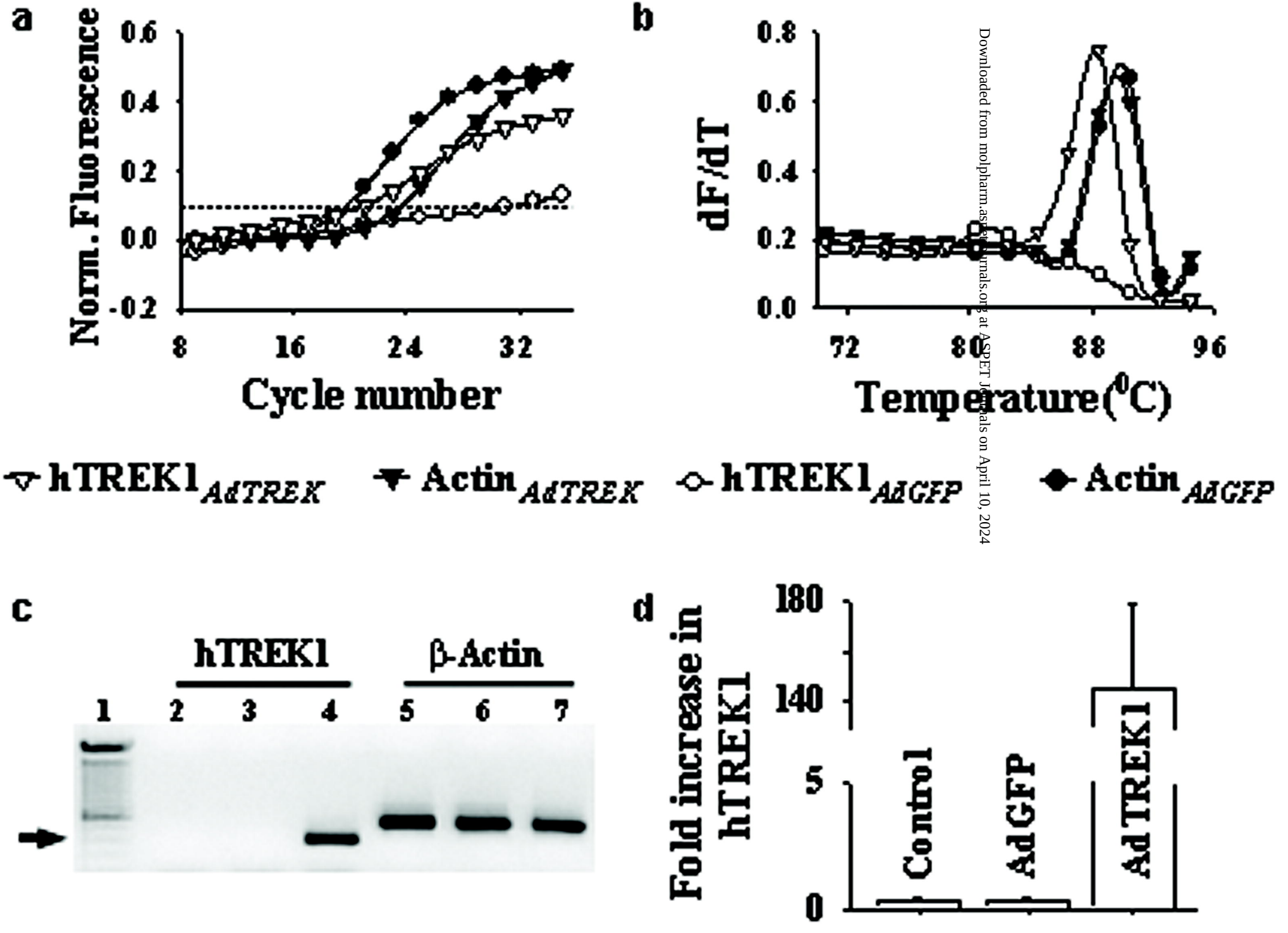

Fig 2

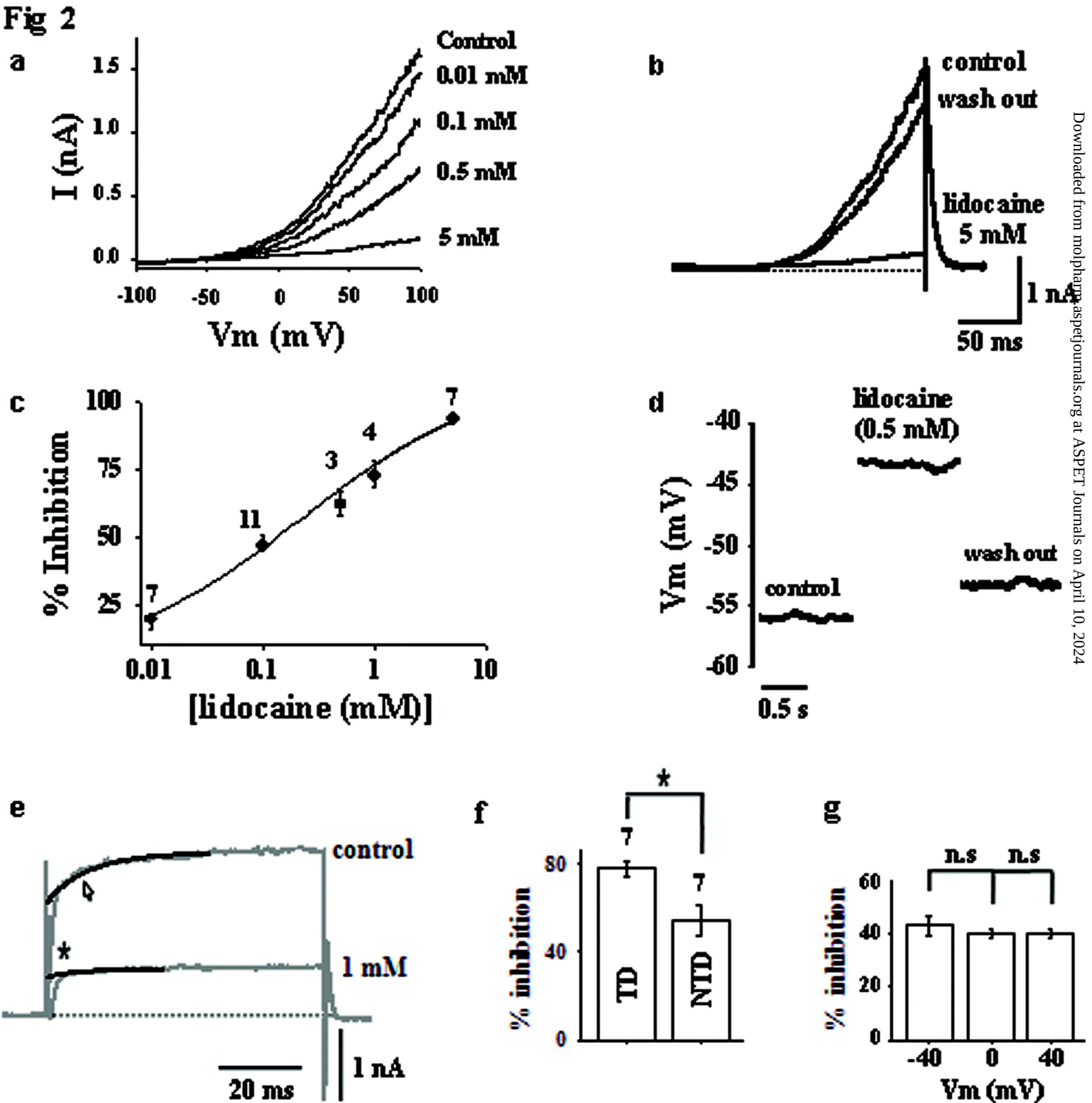

Fig 3

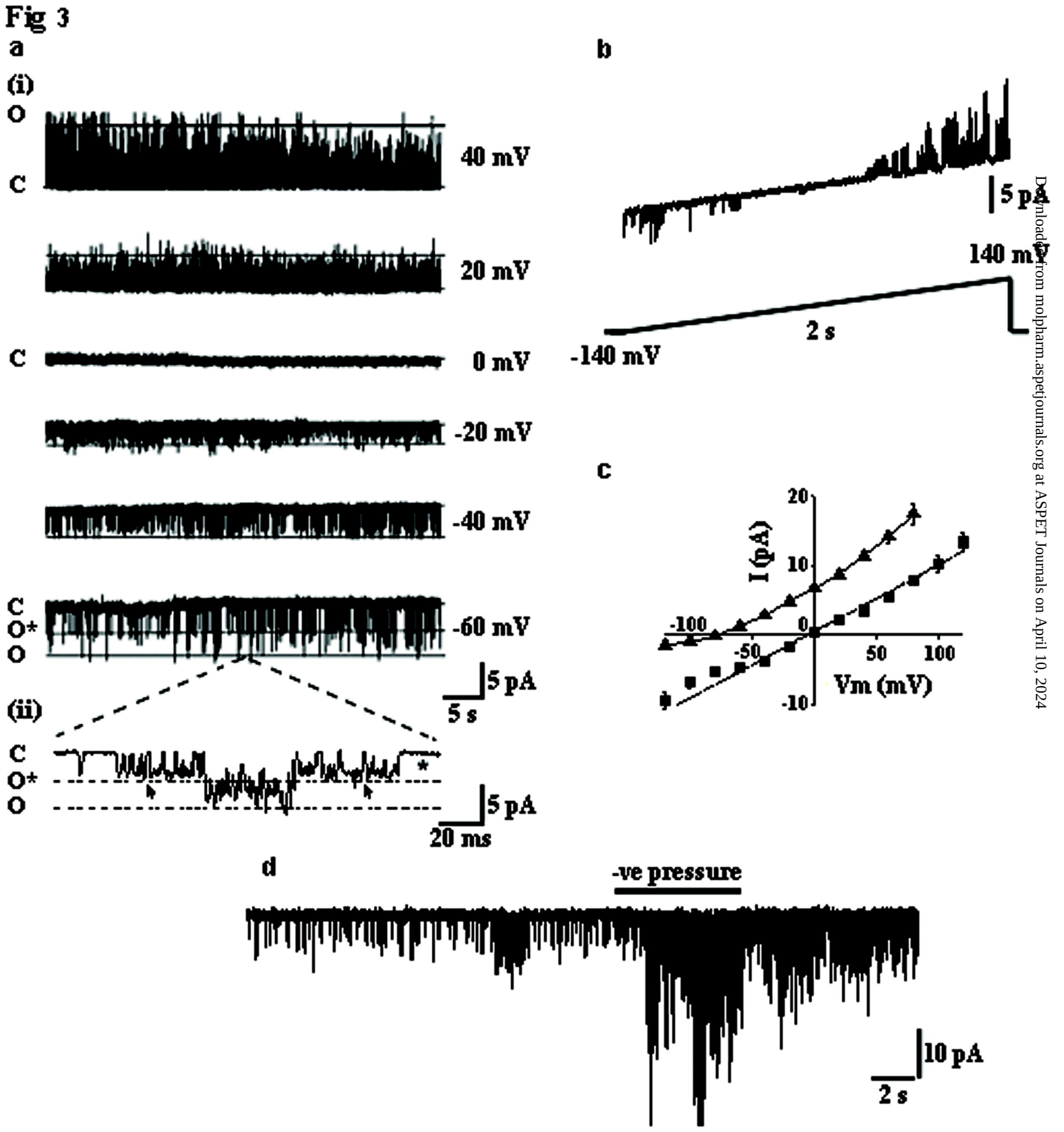

Fig 4

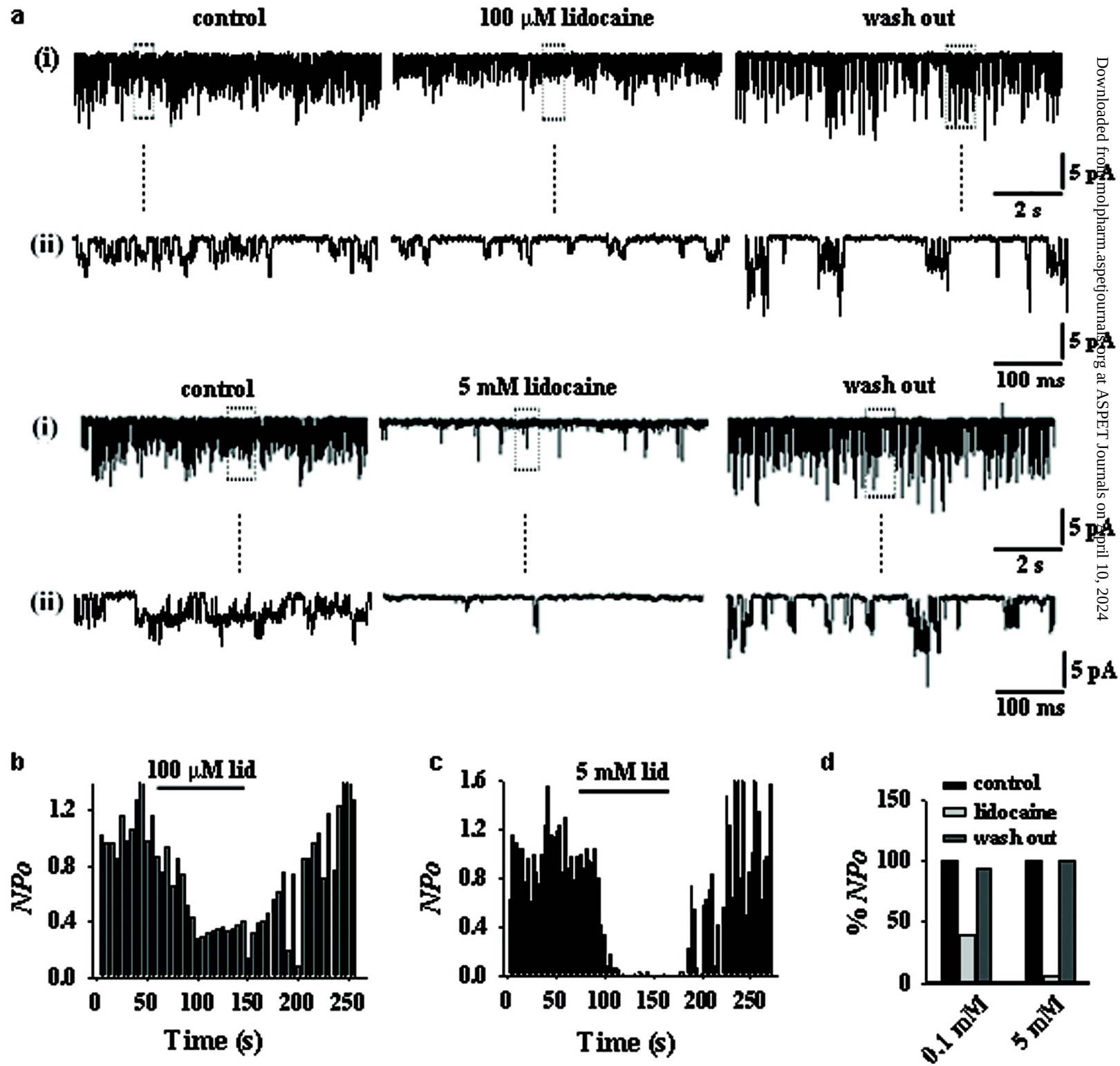

Fig 5

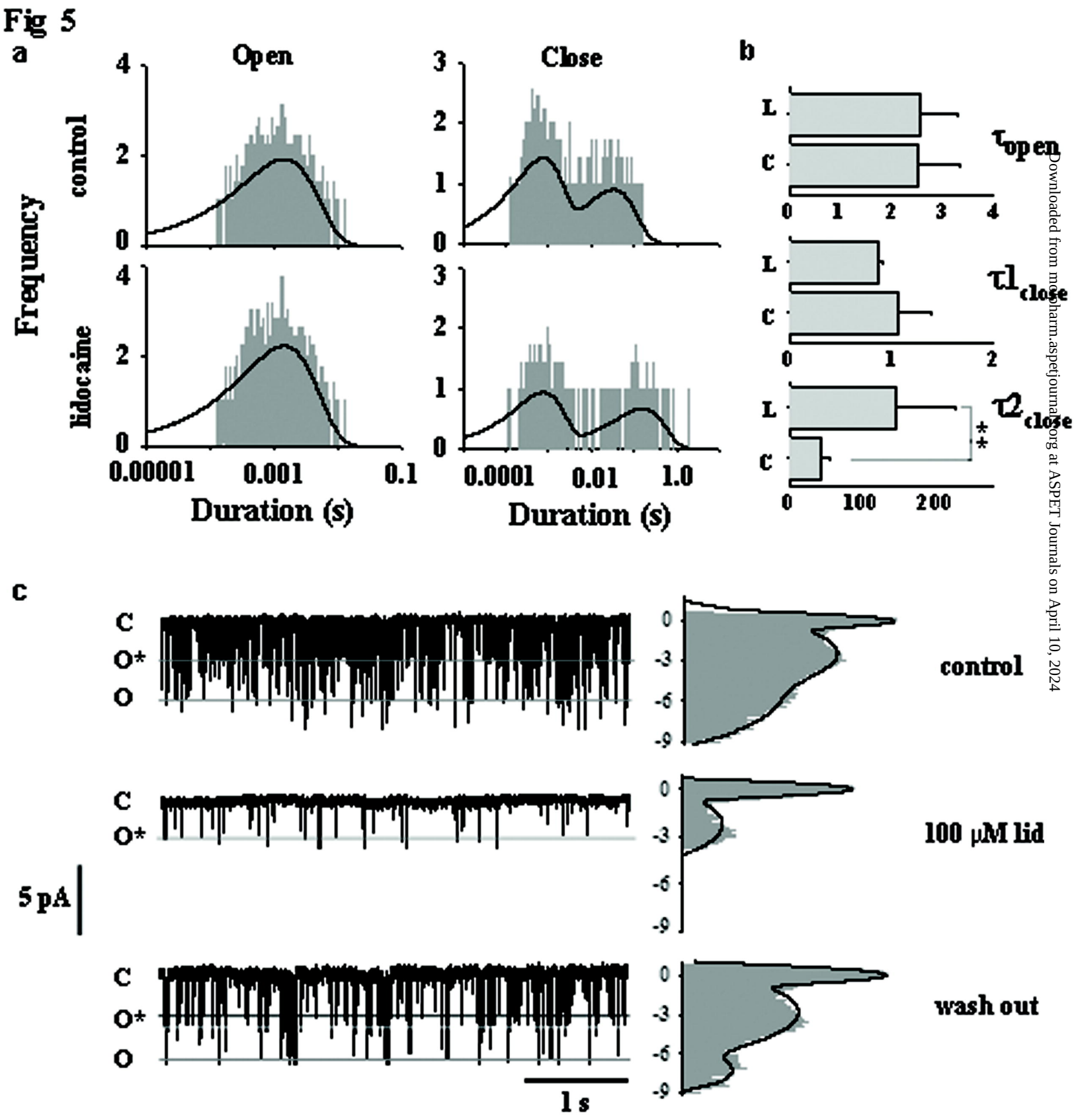

Fig 6

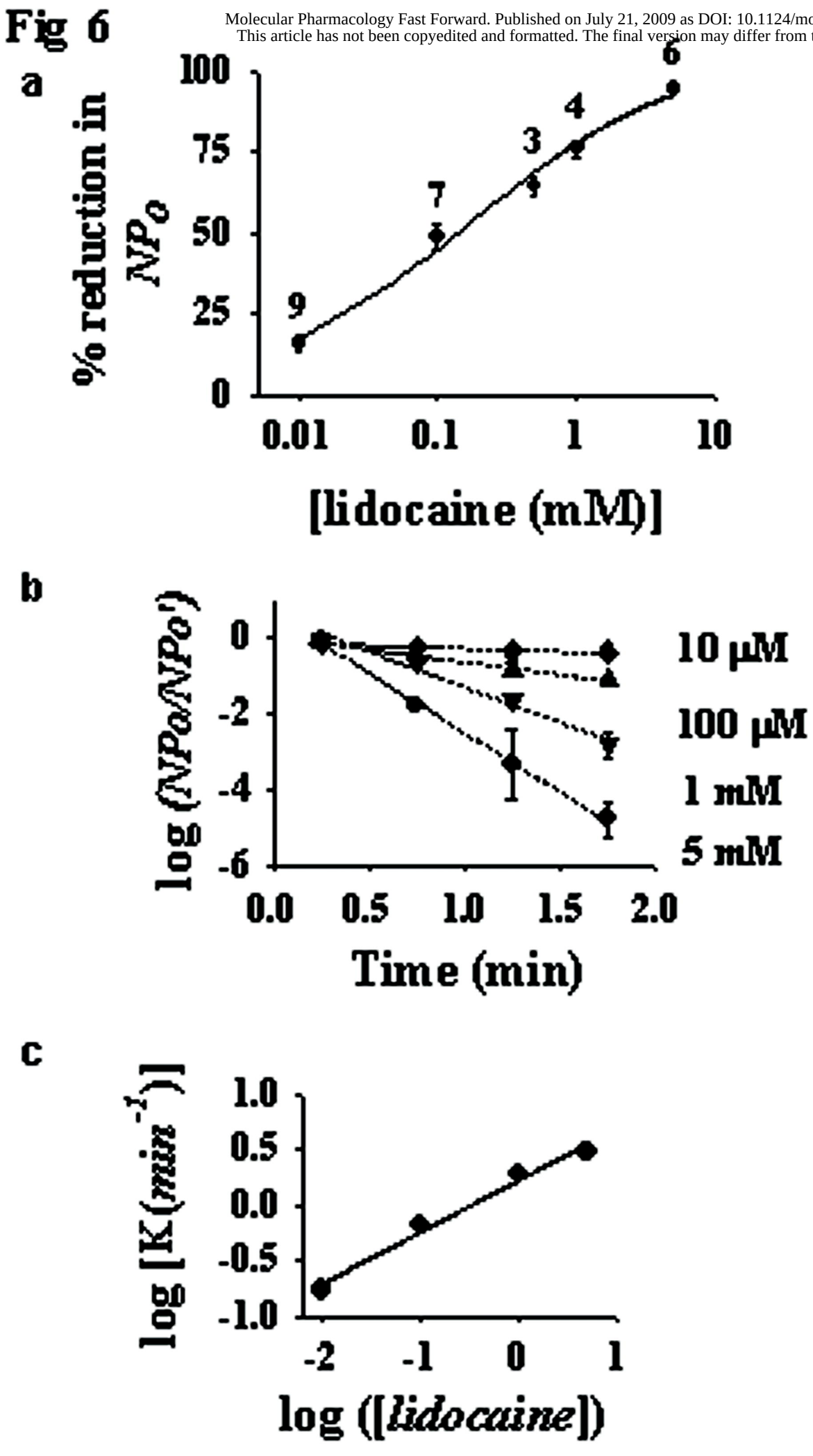

Fig 7

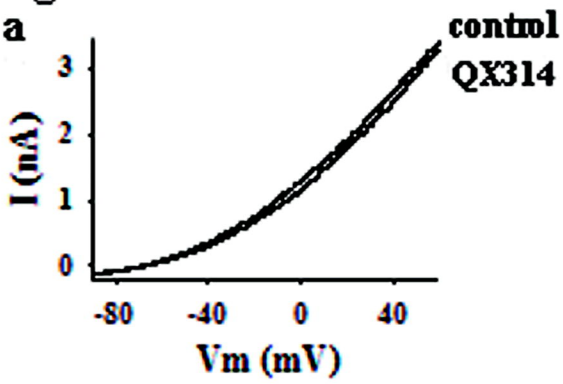

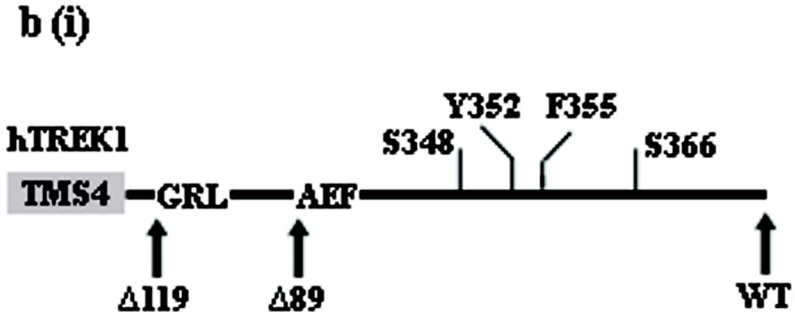

(ii)

```
Q90Z25_9TELE -GIVFFCSYIILSFLVVVNMYIAVILENFNVAQEESSDPLCEDDFQMFDET 1589
SCNA_ELEEL   -GITFFCSYIILSFLVVVNMYIAIILENFGVAQEESSDLLCEDDFVMFDET 1592
SC4AA_DANRE  -GIMFFCSYIIMSFLVVVNMYIAIILENFNNAQEESGDPLCEDDFDMFDET 1589
SC4AA_FUGRU  -GMVFFCSYIIISFLVVVNMYIAIILENFNVAQEESGDVLCEEDFEMFNET 1663
Q9IBF1_TAKPA -GMVFFCSYIIISFLVVVNMYIAIILENFNVAQEESGDVLCEEDFEMFNET 1651
SC4AA_TETNG  -GMMFFCSYIIISFLVVVNMYIAIILENFNVAQEESGDALCEEDFEMFNET 1643
SCN2A_RAT    -GIFFFVSYIIISFLVVVNMYIAVILENFSVATEESAEPLSEDDFEMFYEV 1801
SCN2A_HUMAN  -GIFFFVSYIIISFLVVVNMYIAVILENFSVATEESAEPLSEDDFEMFYEV 1801
SCN4A_HUMAN  -GICFFCSYIIISFLIVVNMYIAIILENFNVATEESSEPLGEDDFEMFYET 1623
hTREK1       STARQFKDYIEVSLRRRTEKFEATVNATWEAAHARFEG-VEEKTKKSIVRV  311
                      * .** :*:    .: : * :  .:  *  .    : *.    : ..
                     355 352 348
                                                        348 352 355
hTREK1_CTD   IGRLVRVISKKTKEEVGEFRAHAAEWTANVTAEFKETRRRLSVEIYDKFQRATSIK 363
hTREK2_CTD   IGDWLRVLSKKTKEEVGEIKAHAAEWKANVTAEFRETRRRLSVEIHDKLQRAATIR 374
             **   :** **********::******.*******:********** **  ***::*:
```

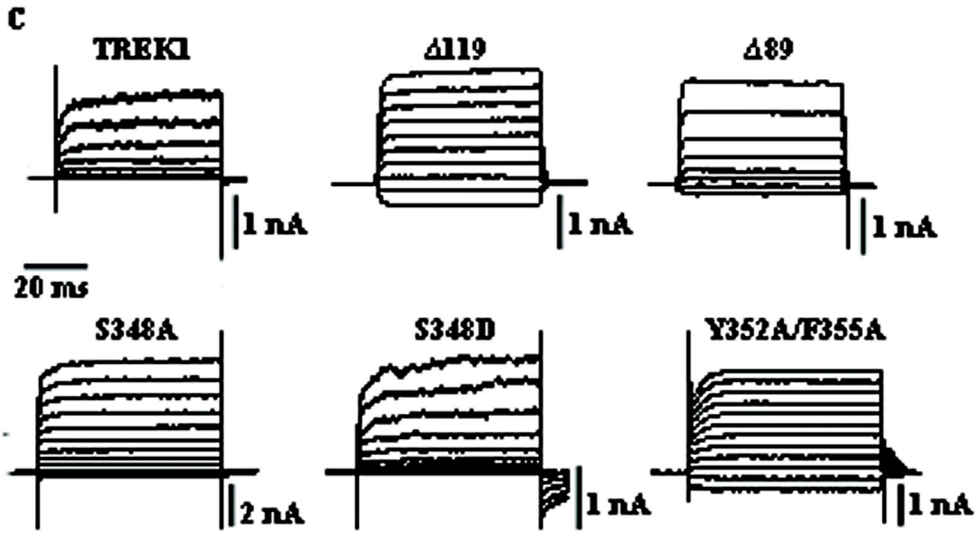

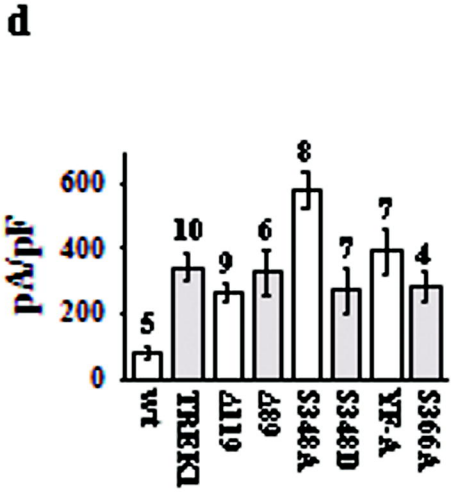

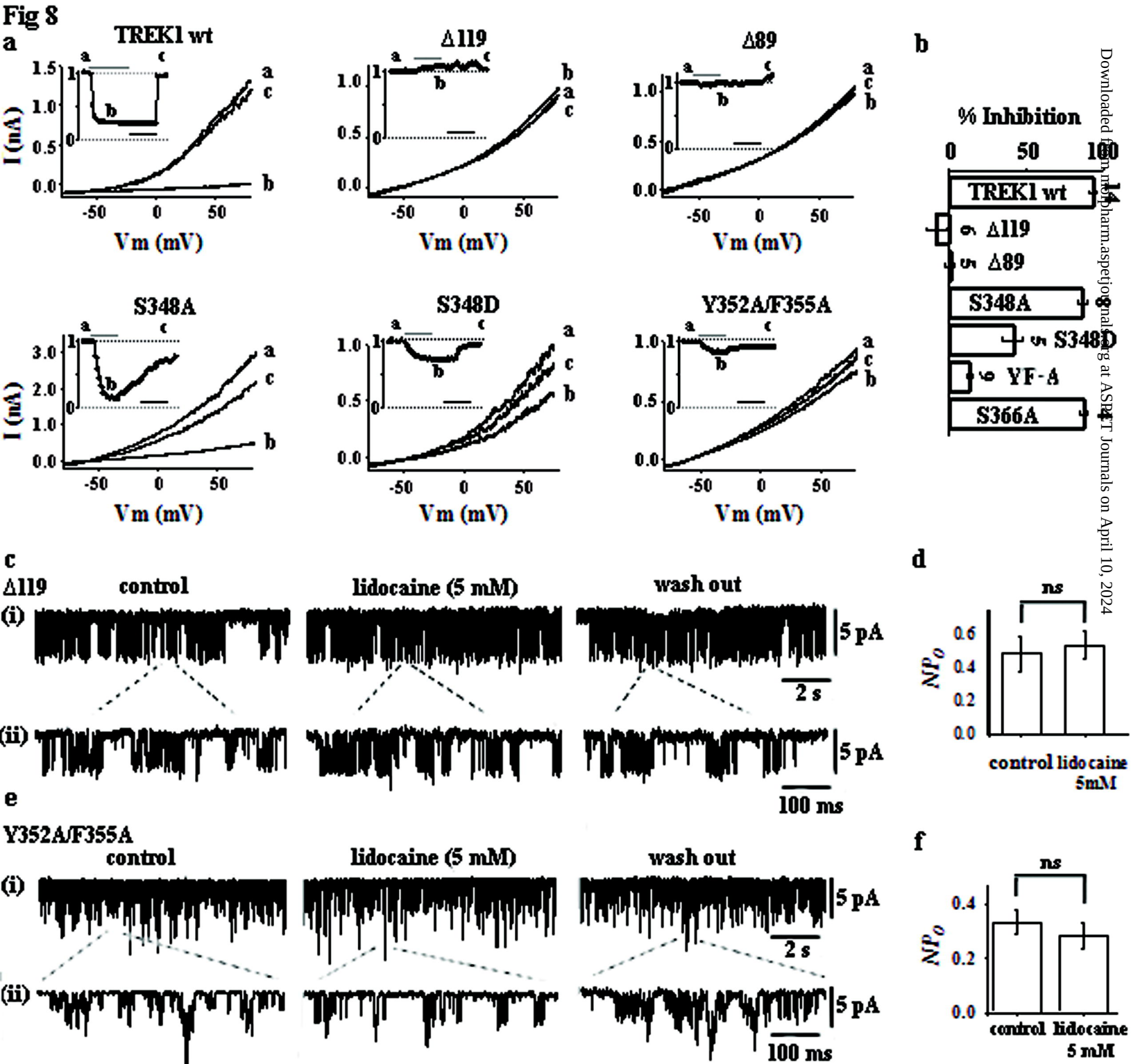

Fig 9

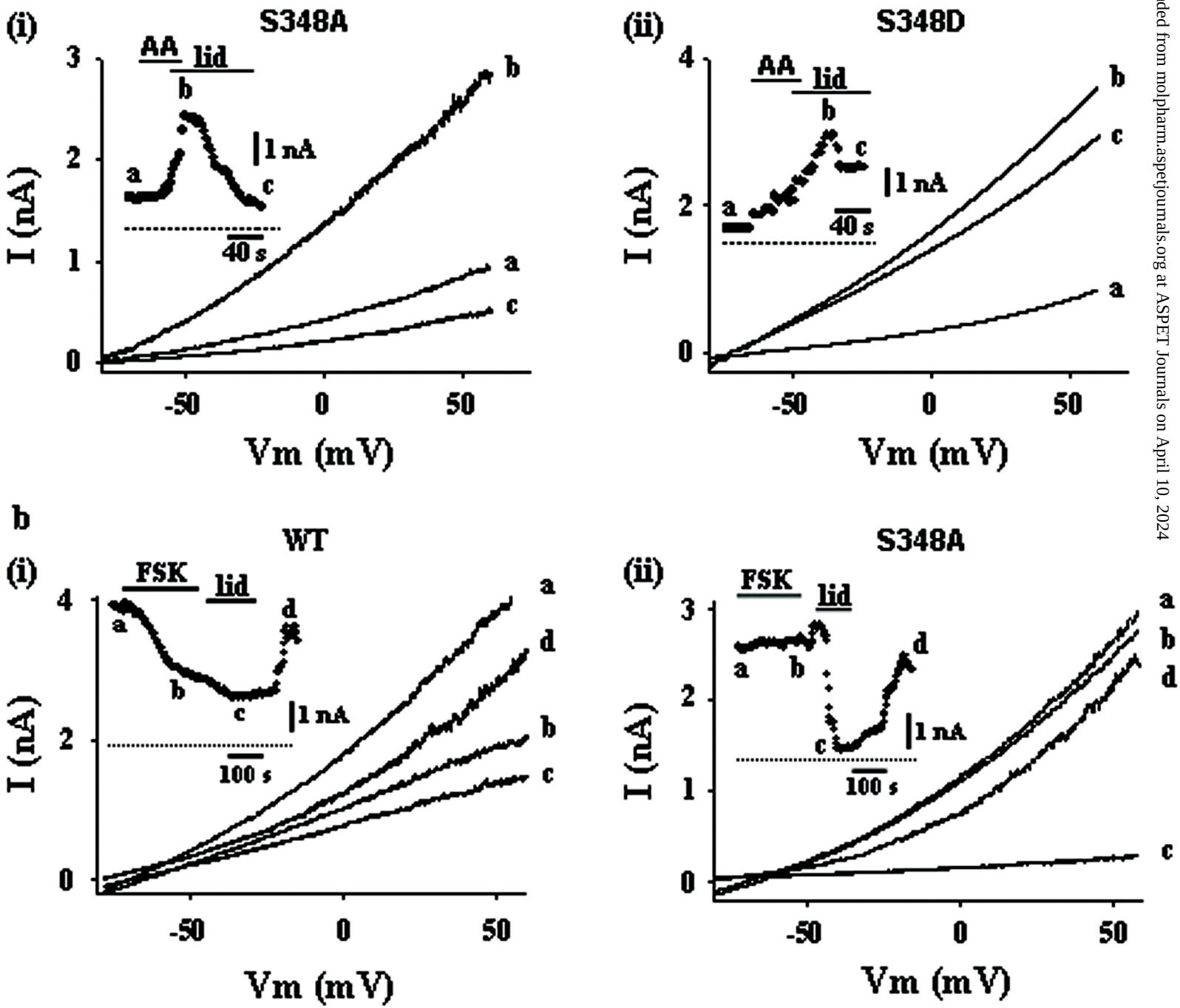

Fig 10

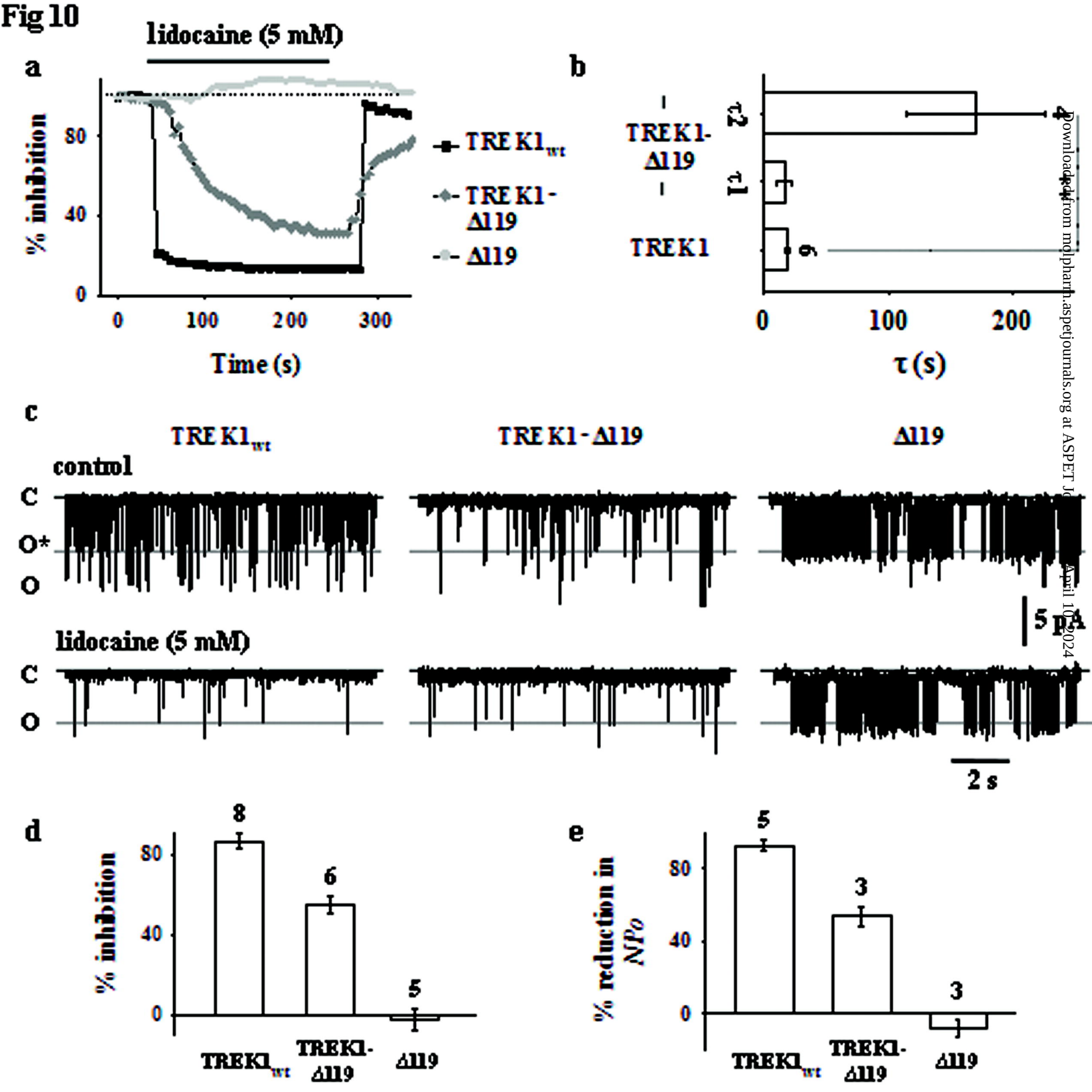

Fig 11

a

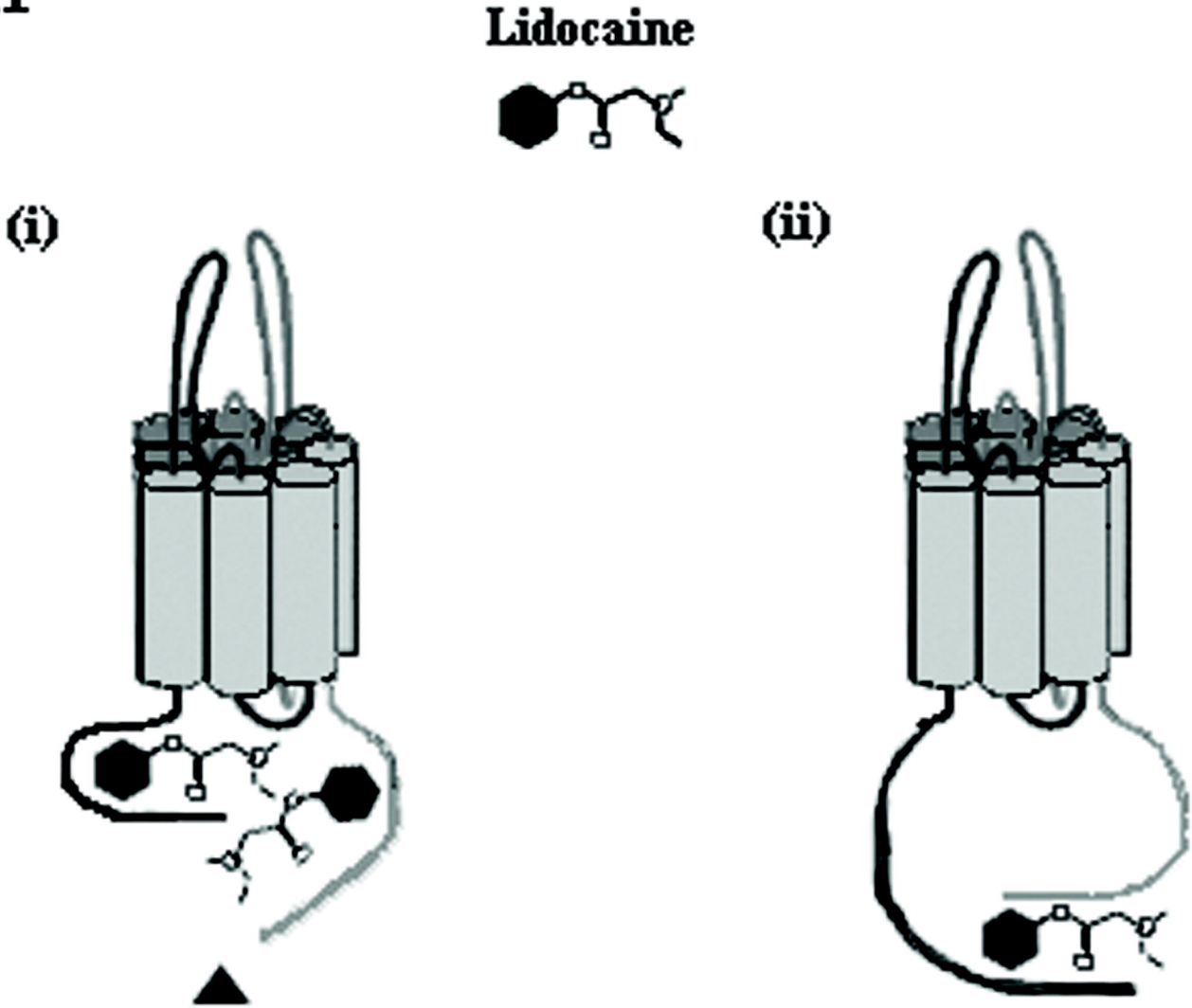

b

$$T \xrightarrow[k1]{L} T.L \underset{k1'}{\overset{L^*}{\rightleftharpoons}} T.LL^* \xrightarrow{k2'} [T\text{-}L]_i'$$

$$T.L \xrightarrow{k2} [T\text{-}L]_i \qquad T.LL^* \xrightarrow{k2''} [T\text{-}L^*]_i'$$